1 **Main Manuscript for**

2 Artificial light at night shifts the circadian system but still leads to physiological

3 disruption in a wild bird

4

5 Davide M. Dominoni[1,2],*, Maaike de Jong[2,3], Kees van Oers[2], Peter O'Shaughnessy[1], Gavin Blackburn[4],

6 Els Atema[2], Christa A. Mateman[2], Pietro B. D'Amelio[5,6,7], Lisa Trost[5], Michelle Bellingham[1], Jessica

7 Clark[1], Marcel E. Visser[2,8], Barbara Helm[1,8]

8

9 [1] Institute of Biodiversity, Animal Health and Comparative Medicine, University of Glasgow,

10 University Avenue, Glasgow, G12 8QQ UK

11 [2] Department of Animal Ecology, Netherlands Institute of Ecology (NIOO-KNAW), Wageningen, The

12 Netherlands

13 [3] Plant Ecology and Nature Conservation Group, Wageningen University & Research, Wageningen,

14 The Netherlands

15 [4] Glasgow Polyomics, Wolfson Wohl Cancer Research Centre, College of Medical, Veterinary and Life

16 Sciences, University of Glasgow, Glasgow G61 1BD, UK

17 [5] Department of Behavioural Neurobiology, Max Planck Institute for Ornithology, Seewiesen,

18 Germany

19 [6] FitzPatrick Institute of African Ornithology, University of Cape Town, Rondebosch 7701, South Africa

20 [7] Centre d'Ecologie Functionnelle et Evolutive, University of Montpellier, CNRS, EPHE, IRD, Univ Paul-

21 Valery Montpellier 3, Montpellier, France

22 [8] Groningen Institute of Evolutionary Life Sciences (GELIFES), University of Groningen, Nijenborgh 7,

23 9747 AG Groningen, The Netherlands

24

25 * Davide M. Dominoni

26   **Email:** davide.dominoni@glasgow.ac.uk

27

28   **Author Contributions:** DMD, MdJ, MEV and BH designed the study. DMD, MdJ, PBD, LT and BH

29   collected the data and samples. DMD, KvO, POS, EA, CAM, MB, JC performed the gene expression

30   assays. GB performed the metabolomics analyses. DMD conducted the statistical analyses. DMD and

31   BH wrote the paper.

32

33   **Competing Interest Statement:** We declare no competing interests.

34   **Classification:** MAJOR: Biological sciences. MINOR: Applied Biological Sciences

35   **Keywords:** light pollution; *Parus major;* circadian disruption; metabolomics; BMAL1.

36   **This PDF file includes:**

37   Main Text

38   Figures 1 to 7

39

40

41

42

43

44

45

46

47

48

49

50

51

Abstract

53 Globally increasing levels of artificial light at night (ALAN) have been associated with shifts in

54 behavioral rhythms of many wild organisms. It is however unknown to what extent this change in

55 behavior is due to shifts in the circadian clock, and, importantly, whether the physiological pathways

56 orchestrated by the circadian clock are desynchronized by ALAN. Such circadian disruption could

57 have severe consequences for wildlife health, as shown for humans. Here, we analyze the effects of

58 experimental ALAN on rhythmic behavior, gene expression and metabolomic profiles in a wild

59 songbird, the great tit (*Parus major*). We exposed 34 captive males to three ALAN intensities or to

60 dark nights and recorded their activity rhythms. After three weeks, we collected mid-day and

61 midnight samples of hypothalamus, hippocampus, liver, spleen and plasma. ALAN advanced wake-up

62 time, and this shift was paralleled by an advance in hypothalamic expression of the clock gene

63 *BMAL1*, which is key to integrating physiological pathways. *BMAL1* advances were remarkably

64 consistent across tissues, suggesting close links of brain and peripheral clock gene expression with

65 activity rhythms. However, only a minority of other candidate genes (4 out of 12) paralleled the

66 shifted *BMAL1* expression. Moreover, metabolomic profiling showed that only 9.7% of the 755

67 analyzed metabolites followed the circadian shift. Thus, despite the shifted timing of key clock

68 functions under ALAN, birds suffered internal desynchronization. We thus suggest circadian

69 disruption to be a key link between ALAN and health impacts, in birds and humans alike.

70

Significance Statement

72 Shifts in daily activity are a common consequence of artificial light at night (ALAN). In humans, shifted

73 activity cycles often become desynchronized from internal physiological rhythms, with serious health

74 implications. To what extent a similar desynchronization occurs in wild animals experiencing ALAN is

75 currently unknown. We exposed captive great tits to increasing levels of LAN, and found that activity

76 patterns and a core clock gene, *BMAL1*, shifted in concert. However, only a minority of additional

77 candidate genes and less than 10% of the metabolites followed this circadian shift, suggesting

78   internal desynchronization of physiological rhythms. Our study emphasizes the massive potential for

79   ALAN to impact the health of wild animals through circadian disruption.

80

Main Text

Introduction

83   On our rhythmic planet, organisms have adapted to the change of day and night by evolving

84   circadian rhythms that are highly sensitive to light (1). The near-ubiquity of circadian rhythms across

85   kingdoms of life suggests major fitness benefits on two grounds. Internally, the circadian system

86   regulates temporal coordination within the body to reduce conflict and overlap between different

87   processes. Externally, the circadian system anticipates environmental fluctuations, enabling

88   organisms to align their behavior and physiology with nature's cycles (1, 2), such as the daily

89   alternation of light and darkness. However, globally most humans and wild organisms in their vicinity

90   are now exposed to artificial light at night (ALAN), and thus to a rapidly altered light environment (3,

91   4) that threatens the refined functioning of the circadian system.

92   In animals, rhythmicity is primarily generated on a molecular level by a transcription-

93   translation feed-back loop (TTFL). This rhythmicity is modulated by multiple interacting systems,

94   including neuronal, endocrine, metabolic and immune pathways (5, 6)(7). The orchestration of these

95   processes involves complex interactions between sensory input, central and peripheral clocks, and

96   effector systems (2). There is increasing evidence that ALAN disrupts these processes, with possible

97   consequences ranging from compromised human health to loss of ecosystem functions (8–10). In

98   free-living and captive organisms, altered daily and annual activity has been widely reported, and

99   experimental illumination has confirmed causal effects of ALAN (11, 12). Still, it is largely unclear

100   whether the circadian system, its multiple components, and the physiological pathways it

101   coordinates, remain synchronized with activity patterns (13–18). ALAN has also been shown to

102   induce physiological changes, including in endocrine, immune and metabolic pathways (15, 19, 20).

103   These changes could be due to circadian disruption, with possible negative consequences for fitness

4

104   (9, 21). Addressing these issues requires multi-level analyses that simultaneously examine effects of

105   ALAN on rhythmic behavior and different physiological pathways (9), but these are currently lacking.

106   Here we aim to fill this gap by an integrated study of a bird, the great tit (*Parus major*),

107   whose behavioral response to ALAN is well-characterized (11, 22–26). We measured day-night

108   differences in gene transcripts in multiple tissues and in blood metabolites under a realistic range

109   (27, 28) of experimental ALAN and in dark controls, and investigated links to behavioral rhythms. The

110   selected genes represented the circadian TTFL (Brain and Muscle ARNT-Like 1, *BMAL1*, alias *ARNTL*;

111   cryptochrome 1, *CRY1*), a clock modulator (*casein kinase 1ε, CK1ε*) (29), and endocrine, immune and

112   metabolic pathways putatively affected by circadian disruption (Table S1). Tissues included central

113   pacemaker and memory sites (hypothalamus, where important avian circadian pacemaker

114   components are located (29), and hippocampus; Fig. S1), and metabolic (liver) and immune tissues

115   (spleen). Testes of the same birds were analyzed in a separate study (30). In contrast to the

116   candidate gene approach, our untargeted metabolomics approach captured both expected and novel

117   effects of ALAN (31). We aimed to identify whether i) hypothalamic clock gene expression was

118   affected by ALAN, ii) potential temporal shifts in clock gene expression were consistent across

119   tissues, iii) behavioral and clock gene rhythms were aligned, and iv) transcript and metabolite

120   temporal shifts were consistent across physiological pathways. Any inconsistencies in temporal shifts

121   indicate the potential for internal desynchronization, and hence, circadian disruption (9, 21).

122   Great tits are a rewarding study system because their urbanized distribution allows to study

123   ALAN responses also in free-living individuals, because detailed molecular and circadian information

124   is available (32–34), and because like humans, they are diurnal (9, 11, 22). We studied 34 male great

125   tits under simulated winter daylength (LD 8.25:15.75 h) in four treatment groups, ranging from dark

126   night controls to 5 lx (Table S2, S3), and sampled metabolites and transcripts at mid-day (3 h 30 min

127   after lights on; i.e. 3.5 h Zeitgeber time) and midnight (7 h 15 min after lights off; i.e. 15.5 h Zeitgeber

128   time). We chose a study design that enabled detection of rhythmicity and ALAN effects from

129   sampling two time-points 12 h apart (35, 36). The design was enhanced firstly by tracking possible

5

130   shifts in circadian rhythms by a focal clock gene, *BMAL1*, whose transcription under dark nights in

131   songbirds peaks in the late evening (29). Secondly, we applied ALAN levels that advance activity of

132   captive great tits by 6 h (22) and thus, if molecular rhythms track behavior, day-night differences at

133   all phase positions are captured.

134   Our specific predictions are illustrated in Figure 1, which shows expected patterns for

135   *BMAL1*. Under dark nights (Fig. 1A, green curve), during midnight sampling (blue dots) *BMAL1*

136   transcripts will have just passed the peak (maximum), and during mid-day (yellow dots) they will

137   have just passed the trough (minimum). Under our hypothesis, the TTFL matches behavior, and thus,

138   with increasing ALAN (red curves), the *BMAL1* rhythm will also advance. Hence, at midnight *BMAL1*

139   levels will be measured progressively later than the peak, and drop, whereas mid-day levels will be

140   measured closer to the next peak, and hence rise. When combining midnight and mid-day data (Fig.

141   1B), we thus expected a cross-over of detected *BMAL1* levels. Other rhythmic compounds should

142   show similar patterns, although the point of intersection and precise change of level depends on

143   their phase. In contrast, if the TTFL does not match the behavioral shift by ALAN, compound levels

144   will show as two horizontal lines across ALAN, representing day and night, respectively. Levels of

145   non-rhythmic compounds will fall on a horizonal line, representing both day and night.

146

Results

ALAN advances circadian timing of activity and BMAL1 expression

149   Daily cycles of activity were strongly affected by the ALAN treatment (GAMM, p=0.001, Fig. 2A and

150   Fig. S2; Table S4). In the 5 lx group birds were generally active 6-7 h before lights-on, whereas birds in

151   the other two light treatments (0.5 and 1.5 lx) advanced morning activity to a much lesser extent.

152   This advancement in the onset of morning activity led to 40% of the overall diel activity in the 5 lx

153   group to occur during the night, compared to 11 and 14% in the 0.5 and 1.5 lx groups, and less than

154   1% in the control dark group. Thus, with increasing ALAN, nocturnal activity also increased (LMM,

155   treatment p < 0.001, Fig. 2A and Table S5).

156   Breaking down this average diel profile (Fig. 2A) by time since first exposure to ALAN (i.e.,

157   days from start of the experiment to first sampling, days 0 to 18) yields insights into how differences

158   in activity developed, and into circadian mechanisms involved (Fig. 2B-C). Upon exposure to ALAN,

159   the birds' activity onset (Fig. 2C) advanced in all treatment groups. In the groups with intermediate

160   light exposure (0.5 lx, 1.5 lx) the phase-advance occurred instantaneously and to a similar extent (155

161   and 142 min for the 0.5 and 1.5 lx groups respectively, P>0.1 for this pairwise comparison), but

162   thereafter timing remained stable. The group exposed to 5 lx showed an even larger instantaneous

163   phase advance of an average of almost five hours (mean ± SEM = 289 ± 21 min), but thereafter

164   continued to gradually phase-advance until reaching a stable phase after 10 days (interaction

165   treatment*day, p< 0.001, Fig. 2C, Table S2). The advance until stabilization could equally represent

166   gradual entrainment to an early phase, or temporary free-run of activity, as suggested by

167   periodogram analysis. Indeed, we found that in the 5 lx group, prior to stabilization, period length

168   deviated from that of all other groups and from 24 h, reaching levels similar to those of free-running

169   conspecifics in an earlier study (37) (mean period length 5 lx group: 23.6 h; LM; Table S6). The

170   individual actograms (Fig. S3) further suggest that the activity rhythm in the 5 lx group may have split

171   into an advancing morning component and a more stably entrained evening component, suggesting

172   internal desynchronization.

173   Changes in the activity offset were much less pronounced (Fig. 2B). The 5 lx group showed an

174   instantaneous phase-shift, which in contrast to morning activity delayed, rather than advanced,

175   activity compared to the lights-off time. This initial delay was followed by a gradual advance of

176   evening offset, similar to but smaller than that of morning onset. At the end of the experiment birds

177   in the 5 lx group ceased their activity before lights-off, and earlier than other groups (treatment*day,

178   p< 0.001, Fig. 2B, Table S5). This advance did not compensate for the earlier onset, as birds in the 5 lx

179   group were more active over the whole 24h than the remaining birds (treatment*day, p= 0.01, Table

180   S5).

181

182 *Hypothalamic BMAL1 expression at night parallels advanced activity onset*

183 We next sought to identify whether the profound shifts in activity patterns were paralleled by

184 corresponding shifts in the pacemaker, measured by expression of *BMAL1* in the hypothalamus. Day-

185 night differences in transcripts of *BMAL1* inverted with increasing ALAN (Fig. S4A), as predicted

186 above (Fig. 1). While *BMAL1* expression was higher at midnight than at mid-day for the control birds,

187 increasing ALAN induced a reversal of this pattern, so that birds in the 5 lx group had much higher

188 expression at mid-day than at midnight (treatment*time, $p < 0.01$, Table S7).

189 To assess whether changes in day-night *BMAL1* gene expression correlated with temporal

190 behavioral shifts, we related *BMAL1* levels to onset of activity of an individual once it had stably

191 shifted in response to the ALAN treatment (Fig. 2B, 2C, after 10 days). Onset was closely predicted by

192 hypothalamic *BMAL1* expression at midnight (Gaussian LM, $p<0.001$, $R^2=0.71$, Fig. 3A). Across ALAN

193 levels, the earliest rising birds had the lowest midnight expression of *BMAL1*. However, the steep

194 linear regression was largely based on differences between ALAN groups in both activity timing (Figs.

195 2, 3) and *BMAL1* expression (Fig. S4A). Indeed, this relationship was even stronger when we only

196 considered the 0.5, 1.5 and 5 lx group in the analysis (Gaussian LM $p<0.001$, $R^2=0.85$), but the

197 association was not present for the dark control birds (Gaussian LM, $P=0.87$). Individual midnight

198 *BMAL1* levels were also predictive of mean offset of activity, albeit less strongly so than for onset

199 (Gaussian LM, $p=0.006$, $R^2=0.28$, Fig. 3B). Conversely, mid-day *BMAL1* levels did not significantly

200 predict variation in any of the activity traits (Gaussian LMs, $p>0.1$ and $R^2<0.16$ for all measures, Fig.

201 3C-D).

202

203 *ALAN reverses day-night BMAL1 expression patterns in multiple tissues*

204 ALAN-induced shifts in *BMAL1,* as detected in the hypothalamus, were remarkably consistent across

205 tissues. Hippocampal *BMAL1* expression profiles resembled those in the hypothalamus (Fig. S5A) and

206 were strongly affected by the interaction of treatment and sampling time ($p<0.001$, Table S8). Within

207 individuals, mid-day and midnight transcripts in both brain tissues were closely related (LM, $p<0.001$,

8

208   Fig. 4A, Table S9). Also liver *BMAL1* showed similar effects of ALAN on day-night expression profiles

209   (Fig. S6A; time*treatment, p<0.001, Table S10), so that within individuals, hepatic and hypothalamic

210   transcripts also correlated closely (LM, p<0.001, Fig. 4B, Table S9). These findings were consolidated

211   by parallel ALAN effects on *BMAL1* expression in the spleen (Fig. S7A; time*treatment, p=0.003,

212   Table S11), and close individual-level correlation of spleen transcripts with those in hypothalamus

213   (LM, p=0.011, Fig. 4C) and liver (LM, p=0.001, Fig. 4D, Table S9).

214

215   ***Partial disruption of expression patterns by ALAN in other genes***

216   We next sought to assess whether the same reversal of day-night expression patterns found

217   for *BMAL1* was paralleled in other genes analyzed in the different tissues. We found mixed evidence

218   for this, as in most of the pathways we examined some genes shifted in concert with *BMAL1*, while

219   others did not. This suggests that different pathways were differentially affected by ALAN.

220   Among clock-related genes, hypothalamic expression levels of *CK1ε*, a clock modulator, was

221   not affected by the light treatment (p=0.71). Expression was consistently, although not significantly,

222   higher at mid-day (p=0.09, Fig. 5H, Table S7). Similarly, the same gene was not significantly affected by

223   sampling time or treatment in the liver. Expression of hepatic *CK1ε* increased with light intensity, albeit

224   not significantly so (p=0.078, Fig. 5P, Table S10), and was not affected by sampling time (p=0.13, Table

225   S10). In the liver another circadian gene, *CRY1*, showed no expression trend that aligned with that of

226   *BMAL1* (Fig. 5O). Moreover, *CRY1* was not affected by treatment or sampling time (P>0.6 for both

227   variables, Fig. 5O, Table S10).

228   Among metabolic genes, patterns similar to those in *BMAL1* were evident in *SIRT1*, a gene

229   which is also involved in the modulation of the circadian cycle (38)(39) (Table S1). Hypothalamic

230   *SIRT1* showed a clear change of day-night expression with increasing ALAN (Fig. 5E; treatment*time,

231   p = 0.029, Table S7), and *SIRT1* mRNA levels were closely related to those of hypothalamic *BMAL1*

232   (LM, p<0.001, Table S9). In the liver, the metabolic gene *NRF1* showed a similar response to ALAN as

233   *BMAL1*, with reversed day-night expression in the 5 lx group compared to other groups

9

234   (treatment*time, p<0.001, Fig. 5F, Table S10), and close correlation with *BMAL1* (LM, p<0.001). In

235   contrast, another hepatic metabolic gene, *IGF1,* was not significantly affected by light treatment or

236   sampling time (for both, p>0.11, Fig. 5Q, Table S10). In the hippocampus (Table S8), mid-day and

237   midnight levels of the mineralocorticoid receptor, *MR*, decreased significantly with increasing ALAN

238   (p=0.044, Fig. 5M). Levels were higher at night than during the day, albeit not significantly so (p=0.1).

239   Last, the levels of the glucocorticoid receptor, *GR*, showed no significant relationship with either light

240   treatment or sampling time (p>0.33 in both cases, Fig. 5N).

241   Among immune genes, ALAN affected the hypothalamic mRNA levels of *LY86*, which showed

242   reduced levels with increasing ALAN (p=0.04, Fig. 5K, Table S7). Expression of this gene tended to be

243   lower at midnight than mid-day, albeit not significantly so (p=0.08). However, the same gene

244   analyzed in the spleen was not affected by either treatment or sampling time (p>0.7, Fig. 5L, Table

245   S11). Conversely, another immune gene in the spleen, *TLR4,* showed the same pattern as *BMAL1* (Fig.

246   5G, time*treatment, p=0.006, Table S11).

247   Last, we also analyzed genes involved in photoperiod seasonal response in the avian brain.

248   *FOXP2*, a gene that in birds is involved in learning, song development and photoperiod-dependent

249   seasonal brain growth, showed no significant trends related to ALAN or sampling time (p>0.32 in both

250   cases, Fig. 5J). *DIO2,* a thyroid-axis gene involved in photoperiodic reproductive activation, was also

251   not affected by either ALAN or sampling time (p>0.45 for both variables, Fig. 5I).

252

Metabolomic profiles support only a limited reversal of day-night physiology under ALAN

254   To explore the different impacts of ALAN on whole-body physiology, we carried out

255   untargeted LC-MS metabolomic analysis and obtained abundance values for 5483 compounds. Out of

256   these, 682 were annotated as known metabolites based on accurate mass and predicted retention

257   time (40) and 73 were identified based on accurate mass measurement and matching retention time

258   to a known standard (within 5%), for a total of 755 metabolites. We ran individual linear mixed

259   models for all these 755 metabolites (correcting for false discovery rate at 5%), and found that 44.1%

260   (333) differed significantly by sampling time, with higher levels at mid-day in 197, and higher levels at

261   midnight in 136 (to see all metabolite tables: https://doi.org/10.6084/m9.figshare.12927539.v1). For

262   29 metabolites we found significant effects of treatment (Table S12). The direction of the treatment

263   effect depended on the metabolite considered. In 11 metabolites, levels decreased with ALAN, while

264   in the remaining 18 metabolites an increase was observed when compared to the dark night control

265   group. Finally, 73 (9.7%) of the 755 metabolites showed significant interaction between treatment

266   and sampling time (Fig. 6 and Table S13; 34 of those also differed by sampling time). As this pattern

267   supported reversal of day-night physiology similar to that shown for activity and *BMAL1* expression,

268   these metabolites were selected for subsequent focal analyses (hereafter named "interactive

269   dataset").

270   We dissected variation in the interactive dataset by using two principal component analyses

271   (PCA) on the samples collected at mid-day and midnight (Fig. 6C, D). For mid-day samples, ALAN

272   treatments overlapped considerably (Fig. 6C), although low values of PC1 (26 % of variance

273   explained) aligned with some of the birds in the 1.5 lx and 5 lx treatments. PC1 in the mid-day

274   dataset was heavily loaded with metabolites of Arginine biosynthesis pathway, including L-Arginine,

275   Homoarginine and L-Glutamate, as well as other important amino acids such as L-Threonine, L-Lysine

276   and L-Tyrosine. Conversely, the midnight samples (Fig. 6D) separated clearly between the 5 lx

277   treatment and the remaining groups. In this midnight PCA, PC1 explained 27% of the variance and

278   was heavily loaded with metabolites of the Glutamate and Arginine pathways, as well as with N-

279   acetl-L-aspartate. PC2, which explained 21% of variation, was heavily loaded with fatty acids,

280   including Linoleate (to see all factor loading tables:

281   https://doi.org/10.6084/m9.figshare.12927536.v1). The contribution of the Arginine pathway was

282   further confirmed by pathway analysis, conducted with Metaboanalyst (41), which indicated

283   "Arginine biosynthesis" as a highly significant pathway in this interactive dataset (p<0.001).

284   "Aminoacyl-tRNA metabolism" (p<0.001), "Histidine metabolism" (p=0.005), and "Alanine, Aspartate

285   and glutamate metabolism" (p=0.026) were also indicated as significant pathways.

11

286   We finally investigated whether, just like midnight levels of *BMAL1* expression (Fig. 4),

287   midnight principal components of metabolites correlated with individual activity timing. PC1 strongly

288   predicted the onset of activity via a linear and quadratic relationship (n = 19, p_{linear} = 0.007,

289    $p_{quadratic}$=0.014, R^2 = 0.92, Fig. 6E), but did not explain offset of activity (p=0.63, R^2 = 0.04, Fig. 6F). PC2

290   was related to neither timing trait (p > 0.2).

291

Discussion

293   Birds advanced the circadian timing of their activity as expected with increasing levels of ALAN, and

294   in parallel the gene expression of our focal clock gene, *BMAL1,* was also advanced in the

295   hypothalamus. Advances in *BMAL1* were consistent across tissues, indicating a shift of the circadian

296   system in tissues implicated in timing, memory, metabolism and immune function. Furthermore,

297   advances in nocturnal *BMAL1* potently correlated with activity onset at the individual level,

298   consolidating close links between core clock gene expression and behavior. Responses of *BMAL1*

299   expression were paralleled by a minority of other genes. Similarly, only 9.7% of the metabolome

300   followed the same shift observed in *BMAL1*, indicating that most physiological pathways were

301   desynchronized from the circadian system. The emerging picture is that birds shifted their internal

302   clock time under ALAN, but suffered a high degree of internal desynchronization.

303   On a behavioral level, our findings closely match those of earlier demonstrations of advanced

304   daily activity under ALAN in captivity for several avian species, including the great tit (15, 22, 24, 42).

305   In the wild, birds also advanced daily activity under ALAN, although to a lesser extent (e.g. (14, 26,

306   43)), and often in onset but not offset (25, 26, 28, 44, 45). Previously, behavioral shifts were

307   interpreted as not involving the circadian clock (24). In an experiment also on the great tit, Spoelstra

308   and colleagues (24) exposed birds to dark nights and then to ALAN as in our study. Subsequently,

309   birds were released to constant low-levels of dim light (0.5 lx), where they free-ran. The study found

310   that the birds free-ran from the timing they had shown under initial dark nights, rather than from

311   their advanced timing under ALAN. Thus, the authors concluded that the behavioral response to

12

312   ALAN was due to masking, while the internal clock remained unchanged (24). Our molecular data

313   suggest a different conclusion, namely that within three weeks of ALAN exposure, internal time had

314   phase-advanced in concert with behavior. These discrepancies are difficult to interpret because

315   inferences of the studies are based on different criteria (molecular vs. behavioral) and different

316   experimental phases (during ALAN vs. during ensuing free-run), but it is clear that additional

317   experimental data are needed.

318   Our transcriptional findings of ALAN-altered rhythmicity gain support from a comparison of

319   clock gene expression in Tree sparrows (*Passer montanus*) from an illuminated urban and dark non-

320   urban habitat (46). Sampled within a day after being brought into captivity, urban birds showed clear

321   advances in the circadian system, including, as in our birds, in hypothalamic *BMAL1*. Other

322   experimental studies have also confirmed effects of ALAN on avian rhythms in brain and other tissues

323   (16, 17). In our study, only some of the investigated regulatory genes aligned with the ALAN-

324   dependent advances of rhythms in behavior and *BMAL1*. The genes from metabolic pathways that

325   have close molecular links to the TTFL, *SIRT1* and *NRF1*, mirrored ALAN-dependent changes in

326   *BMAL1*. However, regulatory genes of immune pathways responded inconsistently, whereby *TLR4*

327   aligned with *BMAL1* whereas *LY86* did not. The learning gene, *FOXP2* and the thyroid-activating gene

328   *DIO2* did not mirror the changes in *BMAL1*, nor did the endocrine genes (*MR, GR, IGF1*). Conversely,

329   in a complementary study on these same birds, we observed that ALAN exposure, which also

330   activated the reproductive system, shifted the day-night expression patterns of corticoid receptors

331   (30).

332   Other experimental studies have confirmed that effects of ALAN on avian rhythms in brain

333   and other tissues differed between genes and pathways. For example, a study on Zebra finches

334   (*Taeniopygia guttata*) reported ALAN-induced changes in rhythmic expression of hypothalamic *CRY1*

335   but not *BMAL1* (16). This differs from our findings, where advances in *BMAL1* were not paralleled by

336   *CRY1* (17), and from findings that *BMAL1* and *CRY1*, but not another TTFL gene, *CLOCK*, advanced in

337   an urban bird (47). Divergent responses between clock genes might participate in circadian

13

338 disruption, and could underlie discrepant behavioral responses, such as differences between activity

339 onset and offset observed in our study, and in wild great tits (25, 26, 44) and other avian species (28,

340 45). In our study in the 5 lx group, we also observed splitting of rhythms, which has previously been

341 linked to reproductive activation (48), a known side-effect of ALAN (13).

342   Our metabolomic data corroborated our main findings on gene expression. Of the 755

343 identified metabolites, nearly 50% (333) differed between mid-day and mid-night levels. However,

344 less than 10 % showed changes in rhythm under ALAN (Fig. 7). These findings confirm that some, but

345 not all featured pathways aligned with shifts in behavior and *BMAL1*. Our findings from captive wild

346 birds under ALAN match those from human studies. To identify the mechanisms by which circadian

347 disruption drives metabolic disorders and other pathologies, these studies severely disrupted the

348 circadian system by sleep deprivation and shift-work protocols (31, 49, 50). The reported changes in

349 gene expression and metabolite levels were similar to those of our birds under ALAN, including highly

350 responsive pathways and compounds, in particular Arginine (50), an amino acid strongly linked to

351 circadian rhythms and innate immune responses (51). Glutamate production from arginine is well

352 known (52), and changes in these two metabolites may be due to changes in energy requirements at

353 the different light intensities. N-acetyl-aspartate, a metabolite involved in energy production from

354 glutamate (53), was also observed to follow changes in behavior and *BMAL1*. Both glutamate and

355 arginine have a variety of biochemical roles (54, 55), so further work would be required to determine

356 which of these functions, if any, are associated to the behavioral and gene expression changes we

357 observed. While preliminary, this data shows the potential of metabolomic techniques for furthering

358 this area of research.

359   Despite our sampling design of only two time-points and low sample sizes, we derived

360 descriptors of internal time (*BMAL1* expression; metabolomics PC1 of interactive dataset) whose

361 midnight levels had high predictive power of activity timing. Thereby, we have shown that internal

362 time can be captured in birds by a single sample of blood or tissue, a frontline ambition of biomedical

363 research (35, 36). Our predictive power was limited to treatment groups and within-ALAN

14

364   individuals, whereas birds kept under dark nights were highly synchronized to the sudden switch of

365   lights-on.

366   For wild animals, our study adds to emerging evidence of detrimental effects of ALAN on

367   physiological pathways (9, 10, 21). For example, under ALAN molecular markers for sleep deprivation

368   were elevated, hypothalamic expression of genes such as *TLR4* was altered (16), neuronal features in

369   the brain were changed, and cognitive processes and mental health-like states were impaired (16,

370   20, 56, 57). Altered hepatic expression of several metabolic genes further suggested negative effects

371   on gluconeogenesis and cholesterol biosynthesis (15). Consequences of ALAN-induced changes in

372   immune function include increased host competence for infectious disease (58), indicating how

373   effects on individuals may cascade to ecological or epidemiological scales.

374   Addressing effects of ALAN is therefore urgent (10, 59). Our data contribute to the rising

375   evidence for dose-dependent responses of behavior and physiology (22, 30, 60), which might allow

376   mitigating against ALAN impacts on wildlife by reducing light intensity (61). Importantly, we detected

377   substantial effects even at light intensities (0.5 lx) that are typically far exceeded by street

378   illumination, and to which animals are exposed to in the wild (27, 28). These findings transfer to

379   other organisms including plants, insects, and mammals including humans (12, 62–65) and call for

380   limits to the ever faster global increase in light pollution (3).

381

382

383   **Materials and Methods**

384   *Data availability*

385   The full details of our methods are presented in the *Supporting* Information document. Raw data,

386   created datasets and R scripts are available via Figshare:

387   (https://figshare.com/projects/Artificial_light_at_night_shifts_the_circadian_system_but_still_leads

388   _to_physiological_disruption_in_a_wild_bird/88841).

389

15

390 *Animals and experimental design*

391 We studied 34 hand-raised, adult male great tits that were kept in individual cages (90 × 50 × 40 cm)

392 under simulated natural daylength and ambient temperature of 10 to 14 ºC with *ad libitum* access to

393 food and water, as described in (30).

394   The experiment started on February 1st, 2014, when daylength was fixed at 8 h 15 min light

395 and 15 h 45 min darkness. During the day, all birds were exposed to full spectrum daylight by high

396 frequency fluorescent lights emitting ~1000 lx at perch level (Activa 172, Philips, Eindhoven, the

397 Netherlands). During the night, birds were assigned to four treatment groups exposed to nocturnal

398 light intensity of 0 lx (n= 13), 0.5 lx (n = 7), 1.5 lx (n = 7), or 5 lx (n = 7). In composing these groups, we

399 prioritized assigning birds to the dark night group to obtain reliable benchmark data on day-night

400 differences in gene expression. Lights were provided by warm white LED light (Philips, Eindhoven,

401 The Netherlands; for details on the spectral composition of lights, see (22)).

402   On Feb 20th an initial blood sample (~200 μl) was collected from all birds at mid-day for

403 metabolomic profiling. On Feb 22nd birds were randomly assigned to mid-day or midnight groups for

404 culling to collect tissues for morphological and molecular analyses. The mid-day group was culled on

405 Feb 22nd, whereas culling of the midnight group was divided over two subsequent nights (Feb 22nd:

406 12 birds; Feb 23rd: 10 birds). Blood was again collected for metabolomic profiling.

407   All experimental procedures were carried out under license NIOO 13.11 of the Animal

408 Experimentation Committee (DEC) of the Royal Netherlands Academy of Arts and Sciences.

409

410 *Locomotor activity*

411 Daily activity patterns of each individual bird were measured continuously using micro-switches

412 recorded by a computer, as described in de Jong et al (22). See Supporting Information for more

413 details.

414

415

16

416   *Gene expression analyses*

417   After culling, organs were extracted, snap-frozen on dry ice, and stored at −80 ºC within 10 min of

418   capture.

419   Brain tissue was cut on a cryostat at – 20 ºC. We cut sagittal sections throughout the brain

420   (Fig. S1). The hypothalamus and hippocampus were located by the use of the Zebrafinch atlas ZEBrA

421   (Oregon Health & Science University, Portland, OR, USA; http://www.zebrafinchatlas.org) and

422   isolated from the frozen brain sections either by surgical punches for the hypothalamus (Harris Uni-

423   Core, 3.0 mm), or by scraping the relevant tissue with forceps, for the hippocampus. For the

424   hypothalamus, the edge of the circular punch was positioned adjacent to the midline and ventral

425   edge of the section, just above the optic chiasm, following the procedure of (66). Hypothalamic and

426   hippocampal tissue was then immediately added to separate 1.5ml buffer tubes provided by the

427   Qiagen RNeasy micro extraction kit (see below), homogenized and stored at -80 °C until extraction.

428   Whole spleens were homogenized with a ryboliser and added to 1.5 ml RNeasy micro buffer

429   and stored at -80 °C. For livers, we cut 0.5 g of tissue from each individual liver, homogenized it and

430   added it to 1.5 ml RNeasy micro buffer and stored it at -80 °C. RNA was extracted using the RNeasy

431   micro extraction kit and reverse transcribed it to generate cDNA using a standard kit following the

432   manufacturer's instructions (Superscript III, Invitrogen).

433   We selected exemplary genes known to be involved in circadian timing, seasonal timing, and

434   in metabolic, immune and endocrine function (Table S1). We analyzed the core clock gene *BMAL1* in

435   all tissues as our primary clock indicator because of the timing of its expression and because of its

436   role as central hub for inter-linking molecular pathways (7). We also studied a second core clock

437   gene, *CRY1*, in a single tissue, and a clock modulator, *CK1ε*, in two tissues. In the hypothalamus, we

438   also studied two genes involved in seasonal changes (*DIO2, FOXP2*), and one metabolic and ageing

439   gene (*SIRT1*). The second metabolic gene, *NRF1*, was studied in the liver. Two immune genes

440   represented different pathways (*LY86, TLR4*). Finally, we studied endocrine genes involved in stress

441   signaling in the Hippocampus (*NR3C1 (alias GR), NR3C2 (alias MR)*) and in tissue homeostasis (*IGF1*),

17

442   as well as reference genes (for full details see Table S1). Primers were built based on the great tit

443   reference genome build 1.1 (https://www.ncbi.nlm.nih.gov/assembly/GCF_001522545.2) (33) and

444   annotation release 101 (https://www.ncbi.nlm.nih.gov/genome/annotation_euk/Parus_major/101/).

445   Primer design was conducted with Geneious version 10.0.2 (67).

446   Amplification efficiency of each primer pair was determined through quantitative real-time

447   polymerase chain reaction (RT-qPCR). RT-qPCR was performed on duplicate samples by a 5-point

448   standard curve. We used reference gene levels to correct for variation in PCR efficiency between

449   samples. Reference gene expression stability was calculated using the application geNorm (68), from

450   which we identified the best pair of reference genes for each tissue. Absolute amounts of cDNA were

451   calculated by conversion of the Ct values ($C \times E^{-Ct}$, with $C=10^{10}$ and $E=2$) (69). The absolute amounts of

452   the candidate genes were then normalized by division by the geometric mean of the absolute

453   amounts of the reference genes. This step yielded relative mRNA expression levels of the candidate

454   genes. For more details, see the Supporting Information document.

455

456   *Metabolomics analysis*

457   See Supporting information for initial sample preparation and for additional details. All samples were

458   analyzed on a Thermo Scientific QExactive Orbitrap mass spectrometer running in positive/negative

459   switching mode. Mass spectrometry data were processed using a combination of XCMS 3.2.0 and

460   MZMatch.R 1.0–4 (70). Unique signals were extracted using the centwave algorithm (71) and

461   matched across biological replicates based on mass to charge ratio and retention time. The final peak

462   set was converted to text for use with IDEOM v18 (72), and filtered on the basis of signal to noise

463   score, minimum intensity and minimum detections, resulting in a final dataset of 755 metabolites.

464

465

466

467

468   *Statistical analysis*

469   All statistical analyses were conducted in R, version 3.63 (73). In all models we included treatment as

470   log-transformed light intensity (adding a constant to avoid zero). Details of all statistical analyses can

471   be seen in the Supporting Information document.

472   To analyze locomotor activity data (i.e. perch-hopping), we first divided the time series of

473   activity into an unstable phase and stable phase (see Supporting information). We used the data in

474   the unstable phase to quantify circadian period length (tau) for each bird, then tested treatment

475   effects using a gaussian linear model (LM). The data in the stable phase were used to test for

476   variation in the proportion of time spent active every hour depending on treatment, using a

477   generalized additive mixed model (GAMM). Finally, we tested for variation in onset time, offset time,

478   nocturnal activity and total daily activity using separate linear mixed models (LMMs).

479   To examine variation in relative transcript levels, we ran LMs including ALAN treatment,

480   sampling time (two-level factor, day and night), and their interaction as explanatory variables, and

481   mRNA expression levels of the different genes in the different tissues as response variables. Similar

482   models were used to test for relationships in mRNA levels between the same gene in different

483   tissues, or different genes in the same tissue.

484   To test for variation in the levels of the individual metabolites identified by the LC-MS, we

485   used all data, including the replicated mid-day samples (total n = 64). We ran independent LMMs for

486   each metabolite, with metabolite levels as response variable (log transformed and normalized), and

487   treatment, time of day and their interaction as explanatory variables. Moreover, we ran two principal

488   component analyses using only the 73 metabolites found to be significantly affected by the

489   treatment*time interaction in the LMMs described above. The two PCAs were run separately for the

490   individual samples collected at mid-day or midnight. We then used the first two principal

491   components (PC1 and PC2) of the midnight based PCA as explanatory variables in two LMs with onset

492   and offset of activity as response variables, respectively.

493

19

Acknowledgments

References

1. R. G. Foster, L. Kreitzmann, *Rhythms of life: The biological clocks that control the daily lives of every living thing* (Yale University Press, 2004).

2. B. Helm, *et al.*, Two sides of a coin: Ecological and chronobiological perspectives of timing in the wild. *Philos. Trans. R. Soc. B Biol. Sci.* **372** (2017).

3. F. Falchi, *et al.*, The new world atlas of artificial night sky brightness. *Sci. Adv.* **2**, e1600377–e1600377 (2016).

4. T. W. Davies, T. Smyth, Why artificial light at night should be a focus for global change research in the 21st century. *Glob. Chang. Biol.*, early view (2017).

5. J. C. Borniger, Y. M. Cisse, Surbhi, R. J. Nelson, Reciprocal Regulation of Circadian Rhythms and Immune Function. *Curr. Sleep Med. Reports* **3**, 93–103 (2017).

6. G. Caratti, *et al.*, REVERBa couples the circadian clock to hepatic glucocorticoid action. *J. Clin. Invest.* **128**, 4454–4471 (2018).

7. A. Ribas-Latre, K. Eckel-Mahan, Interdependence of nutrient metabolism and the circadian clock system: Importance for metabolic health. *Mol. Metab.* **5**, 133–152 (2016).

8. D. M. Dominoni, R. J. Nelson, Artificial light at night as an environmental pollutant: An integrative approach across taxa, biological functions, and scientific disciplines. *J. Exp. Zool. Part A Ecol. Integr. Physiol.* **329** (2018).

9. C. Vetter, Circadian disruption: What do we actually mean? *Eur. J. Neurosci.* **51**, 531–550 (2020).

10. J. Falcón, *et al.*, Exposure to Artificial Light at Night and the Consequences for Flora, Fauna, and Ecosystems. *Front. Neurosci.* **14**, 1183 (2020).

11. J. Q. Ouyang, *et al.*, Restless roosts – light pollution affects behavior, sleep and physiology in a free-

522 living songbird. *Glob. Chang. Biol.*, 1–8 (2017).

523 12. E. Knop, *et al.*, Artificial light at night as a new threat to pollination. *Nature* (2017)

524 https:/doi.org/10.1038/nature23288.

525 13. D. Dominoni, M. Quetting, J. Partecke, Artificial light at night advances avian reproductive physiology.

526 *Proc. R. Soc. B Biol. Sci.* **280**, 20123017 (2013).

527 14. D. M. M. Dominoni, B. Helm, M. Lehmann, H. B. B. Dowse, J. Partecke, Clocks for the city: circadian

528 differences between forest and city songbirds. *Proc. R. Soc. London B Biol. Sci.* **280**, 20130593 (2013).

529 15. T. Batra, I. Malik, V. Kumar, Illuminated night alters behaviour and negatively affects physiology and

530 metabolism in diurnal zebra finches. *Environ. Pollut.* **254**, 112916 (2019).

531 16. T. Batra, I. Malik, A. Prabhat, S. K. Bhardwaj, V. Kumar, Sleep in unnatural times: illuminated night

532 negatively affects sleep and associated hypothalamic gene expressions in diurnal zebra finches. *Proc. R.*

533 *Soc. B Biol. Sci.* **287**, 20192952 (2020).

534 17. Y. Yang, Q. Liu, T. Wang, J. Pan, Light pollution disrupts molecular clock in avian species: A power-

535 calibrated meta-analysis. *Environ. Pollut.*, 114206 (2020).

536 18. V. Van Der Vinne, *et al.*, Cold and hunger induce diurnality in a nocturnal mammal. *Proc. Natl. Acad. Sci.*

537 *U. S. A.* **111**, 15256–15260 (2014).

538 19. J. Q. Ouyang, S. Davies, D. Dominoni, Hormonally mediated effects of artificial light at night on behavior

539 and fitness: linking endocrine mechanisms with function. *J. Exp. Biol.* **221**, jeb156893 (2018).

540 20. S. Moaraf, *et al.*, Artificial light at night affects brain plasticity and melatonin in birds. *Neurosci. Lett.*

541 **716**, 134639 (2020).

542 21. C. R. C. Moreno, K. Wright, D. J. Skene, F. M. Louzada, Phenotypic plasticity of circadian entrainment

543 under a range of light conditions. *Neurobiol. Sleep Circadian Rhythm.* **9**, 100055 (2020).

544 22. M. de Jong, *et al.*, Dose-dependent responses of avian daily rhythms to artificial light at night. *Physiol.*

545 *Behav.* **155**, 172–179 (2016).

546 23. J. Sun, T. Raap, R. Pinxten, M. Eens, Artificial light at night affects sleep behaviour differently in two

547 closely related songbird species. *Environ. Pollut.* **231**, 882–889 (2017).

548 24. K. Spoelstra, I. Verhagen, D. Meijer, M. E. Visser, Artificial light at night shifts daily activity patterns but

549 not the internal clock in the great tit (Parus major). *Proc. R. Soc. B Biol. Sci.* **285**, 20172751 (2018).

550 25. Z. N. Ulgezen, *et al.*, The preference and costs of sleeping under light at night in forest and urban great

21

tits. *Proc. R. Soc. B Biol. Sci.* **286**, 20190872 (2019).

26. T. Raap, R. Pinxten, M. Eens, Light pollution disrupts sleep in free-living animals. *Sci. Rep.* **5**, 13557 (2015).

27. D. Dominoni, M. Quetting, J. Partecke, Artificial light at night advances avian reproductive physiology. *Proc. R. Soc. B Biol. Sci.* **280** (2013).

28. D. M. D. Dominoni, E. O. E. Carmona-Wagner, M. Hofmann, B. Kranstauber, J. Partecke, Individual-based measurements of light intensity provide new insights into the effects of artificial light at night on daily rhythms of urban-dwelling songbirds. *J. Anim. Ecol.* **83**, 681–692 (2014).

29. V. M. Cassone, J. K. Paulose, C. E. Harpole, Y. Li, M. Whitfield-Rucker, "Avian circadian organization" in *Biological Timekeeping: Clocks, Rhythms and Behaviour*, (Springer (India) Private Ltd., 2017), pp. 241–256.

30. D. Dominoni, *et al.*, Dose-response effects of light at night on the reproductive physiology of great tits (Parus major): Integrating morphological analyses with candidate gene expression. *J. Exp. Zool. Part A Ecol. Integr. Physiol.* **2018**, 1–15 (2018).

31. S. K. Davies, *et al.*, Effect of sleep deprivation on the human metabolome. *Proc. Natl. Acad. Sci.* **111**, 10761–10766 (2014).

32. H. Watson, E. Videvall, M. N. Andersson, C. Isaksson, Transcriptome analysis of a wild bird reveals physiological responses to the urban environment. *Sci. Rep.* **7**, 1–10 (2017).

33. V. N. Laine, *et al.*, Evolutionary signals of selection on cognition from the great tit genome and methylome. *Nat. Commun.* **7**, 10474 (2016).

34. P. Capilla-Lasheras, *et al.*, Elevated Immune Gene Expression Is Associated with Poor Reproductive Success of Urban Blue Tits. *Front. Ecol. Evol.* **5**, 64 (2017).

35. T. Kasukawa, *et al.*, Human blood metabolite timetable indicates internal body time. *Proc. Natl. Acad. Sci. U. S. A.* **109**, 15036–15041 (2012).

36. E. E. Laing, *et al.*, Blood transcriptome based biomarkers for human circadian phase. *Elife* **6** (2017).

37. B. Helm, M. E. Visser, Heritable circadian period length in a wild bird population. *Proc. R. Soc. B Biol. Sci.* **277**, 3335–3342 (2010).

38. H.-C. Chang, L. Guarente, SIRT1 Mediates Central Circadian Control in the SCN by a Mechanism that Decays with Aging. *Cell* **153**, 1448–1460 (2013).

22

580   39.   A. K. Trivedi, J. Kumar, S. Rani, V. Kumar, Annual life history-dependent gene expression in the

581   hypothalamus and liver of a migratory songbird: Insights into the molecular regulation of seasonal

582   metabolism. *J. Biol. Rhythms* **29**, 332–345 (2014).

583   40.   D. J. Creek, *et al.*, Toward global metabolomics analysis with hydrophilic interaction liquid

584   chromatography-mass spectrometry: Improved metabolite identification by retention time prediction.

585   *Anal. Chem.* **83**, 8703–8710 (2011).

586   41.   J. Chong, *et al.*, MetaboAnalyst 4.0: Towards more transparent and integrative metabolomics analysis.

587   *Nucleic Acids Res.* **46**, W486–W494 (2018).

588   42.   D. M. D. Dominoni, W. Goymann, B. Helm, J. Partecke, Urban-like night illumination reduces melatonin

589   release in European blackbirds (Turdus merula): implications of city life for biological time-keeping of

590   songbirds. *Front. Zool.* **10**, 60 (2013).

591   43.   B. Kempenaers, P. Borgström, P. Loës, E. Schlicht, M. Valcu, Artificial night lighting affects dawn song,

592   extra-pair siring success, and lay date in songbirds. *Curr. Biol.* **20**, 1735–1739 (2010).

593   44.   D. M. Dominoni, J. A. H. Smit, M. E. Visser, W. Halfwerk, Multisensory pollution: Artificial light at night

594   and anthropogenic noise have interactive effects on activity patterns of great tits (Parus major).

595   *Environ. Pollut.*, 113314 (2019).

596   45.   A. Da Silva, J. Samplonius, E. Schlicht, M. Valcu, B. Kempenaers, Artificial night lighting rather than

597   traffic noise affects the daily timing of dawn and dusk singing in common European songbirds. *Behav.*

598   *Ecol.* **25**, 1037–1047 (2014).

599   46.   Z. Renthlei, A. K. Trivedi, Effect of urban environment on pineal machinery and clock genes expression

600   of tree sparrow (Passer montanus). *Environ. Pollut.* **255**, 113278 (2019).

601   47.   Z. Renthlei, B. K. Borah, T. Gurumayum, A. K. Trivedi, Season dependent effects of urban environment

602   on circadian clock of tree sparrow (Passer montanus). *Photochem. Photobiol. Sci.* (2020)

603   https:/doi.org/10.1039/d0pp00257g (December 9, 2020).

604   48.   F. Gwinner, Testosterone Induces "Splitting" of Circadian Locomotor Activity Rhythms in Birds. *Science*

605   *(80-.).* **185**, 72–74 (1974).

606   49.   S. N. Archer, *et al.*, PNAS Plus: From the Cover: Mistimed sleep disrupts circadian regulation of the

607   human transcriptome. *Proc. Natl. Acad. Sci.* **111**, E682–E691 (2014).

608   50.   D. J. Skene, *et al.*, Separation of circadian- and behavior-driven metabolite rhythms in humans provides

23

609   a window on peripheral oscillators and metabolism. *Proc. Natl. Acad. Sci. U. S. A.* **115**, 7825–7830

610   (2018).

611   51.   S. M. Morris, Arginine: Master and commander in innate immune responses. *Sci. Signal.* **3**, pe27–pe27

612   (2010).

613   52.   S. M. Morris, Enzymes of arginine metabolism in *Journal of Nutrition*, (American Institute of Nutrition,

614   2004), pp. 2743S-2747S.

615   53.   J. B. Clark, N-acetyl aspartate: A marker for neuronal loss or mitochondrial dysfunction in

616   *Developmental Neuroscience*, (Dev Neurosci, 1998), pp. 271–276.

617   54.   S. D. Yelamanchi, *et al.*, A pathway map of glutamate metabolism. *J. Cell Commun. Signal.* **10**, 69–75

618   (2016).

619   55.   S. M. Morris, Arginine metabolism revisited. *J. Nutr.* **146**, 2579S-2586S (2016).

620   56.   S. K. T. Taufique, A. Prabhat, V. Kumar, Illuminated night alters hippocampal gene expressions and

621   induces depressive-like responses in diurnal corvids. *Eur. J. Neurosci.* **48**, 3005–3018 (2018).

622   57.   S. K. T. Taufique, A. Prabhat, V. Kumar, Constant light environment suppresses maturation and reduces

623   complexity of new born neuron processes in the hippocampus and caudal nidopallium of a diurnal

624   corvid: Implication for impairment of the learning and cognitive performance. *Neurobiol. Learn. Mem.*

625   **147**, 120–127 (2018).

626   58.   M. E. Kernbach, *et al.*, Light pollution increases West Nile virus competence of a ubiquitous passerine

627   reservoir species. *Proc. R. Soc. B Biol. Sci.* **286**, 20191051 (2019).

628   59.   C. C. M. Kyba, *et al.*, Artificially lit surface of Earth at night increasing in radiance and extent. *Sci. Adv.* **3**,

629   e1701528 (2017).

630   60.   A. Bruening, F. Hölker, S. Franke, T. Preuer, W. Kloas, Spotlight on fish: Light pollution affects circadian

631   rhythms of European perch but does not cause stress. *Sci. Total Environ.* **511**, 516–522 (2015).

632   61.   K. J. Gaston, T. W. Davies, J. Bennie, J. Hopkins, REVIEW: Reducing the ecological consequences of

633   night-time light pollution: options and developments. *J. Appl. Ecol.* **49**, 1256–1266 (2012).

634   62.   D. Dominoni, J. Borniger, R. Nelson, Light at night, clocks and health: from humans to wild organisms.

635   *Biol. Lett.* **12**, 20160015 (2016).

636   63.   J. Bennie, T. W. Davies, D. Cruse, K. J. Gaston, Ecological effects of artificial light at night on wild plants.

637   *J. Ecol.* **104**, 611–620 (2016).

24

638   64.   F. van Langevelde, *et al.*, Declines in moth populations stress the need for conserving dark nights. *Glob.*

639   *Chang. Biol.* **24**, 925–932 (2018).

640   65.   D. Paksarian, *et al.*, Association of Outdoor Artificial Light at Night with Mental Disorders and Sleep

641   Patterns among US Adolescents. *JAMA Psychiatry* (2020)

642   https:/doi.org/10.1001/jamapsychiatry.2020.1935 (August 27, 2020).

643   66.   N. Perfito, *et al.*, Anticipating spring: Wild populations of great tits (Parus major) differ in expression of

644   key genes for photoperiodic time measurement. *PLoS One* **7** (2012).

645   67.   M. Kearse, *et al.*, Geneious Basic: An integrated and extendable desktop software platform for the

646   organization and analysis of sequence data. *Bioinformatics* **28**, 1647–1649 (2012).

647   68.   J. Vandesompele, *et al.*, Accurate normalization of real-time quantitative RT-PCR data by geometric

648   averaging of multiple internal control genes. *Genome Biol.* **3**, research0034.1 (2002).

649   69.   F. Dijk, E. Kraal-Muller, W. Kamphuis, Ischemia-Induced Changes of AMPA-Type Glutamate Receptor

650   Subunit Expression Pattern in the Rat Retina: A Real-Time Quantitative PCR Study. *Investig.*

651   *Ophthalmol. Vis. Sci.* **45**, 330–341 (2004).

652   70.   R. A. Scheltema, A. Jankevics, R. C. Jansen, M. A. Swertz, R. Breitling, PeakML/mzMatch: A file format,

653   Java library, R library, and tool-chain for mass spectrometry data analysis. *Anal. Chem.* **83**, 2786–2793

654   (2011).

655   71.   R. Tautenhahn, C. Bottcher, S. Neumann, Highly sensitive feature detection for high resolution LC/MS.

656   *BMC Bioinformatics* **9**, 1–16 (2008).

657   72.   D. J. Creek, A. Jankevics, K. E. V. Burgess, R. Breitling, M. P. Barrett, IDEOM: An Excel interface for

658   analysis of LC-MS-based metabolomics data. *Bioinformatics* **28**, 1048–1049 (2012).

659   73.   R Development Core Team, R: A language and environment for statistical computing. *URL http//www.*

660   *R-project. org* (2015).

661 **Figures and Tables**
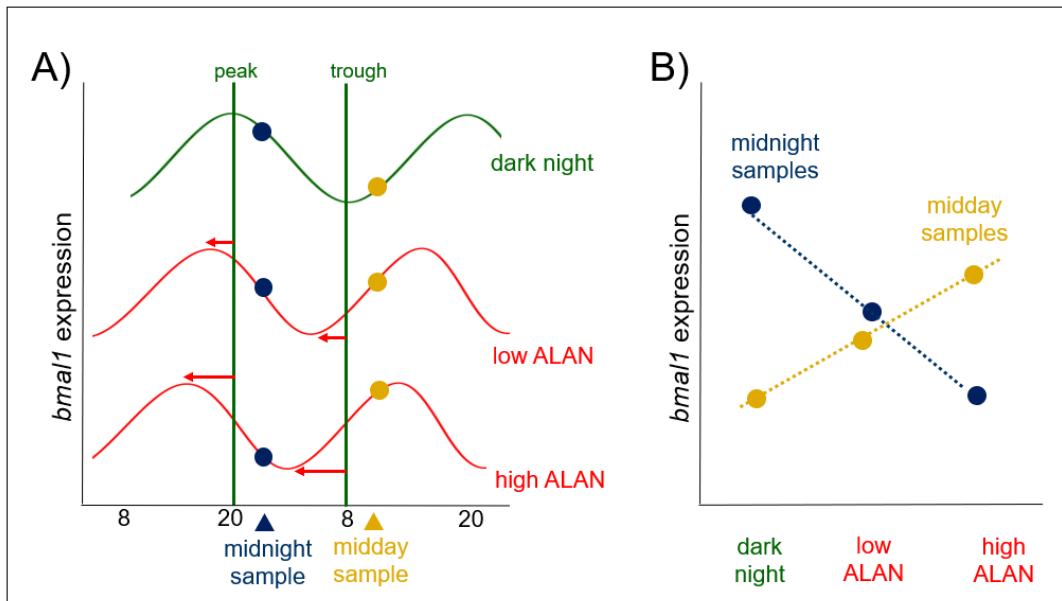
662

663 **Figure 1. Expected clock gene rhythm advance in response to ALAN.** Schematic shows ALAN effects

664 on transcript levels of *BMAL1* measured at midnight (blue) and mid-day (yellow). (A) Rhythm of ALAN

665 under dark night shown as green curve; if the gene's rhythm advances (red curves) with increasing

666 ALAN, transcript levels sampled at midnight will drop, whereas those measured at mid-day will rise;

667 horizontal arrows indicate the advance of the *BMAL1* peak. (B) The trends of transcripts with

668 increasing ALAN therefore cross for mid-day vs. midnight sampling.
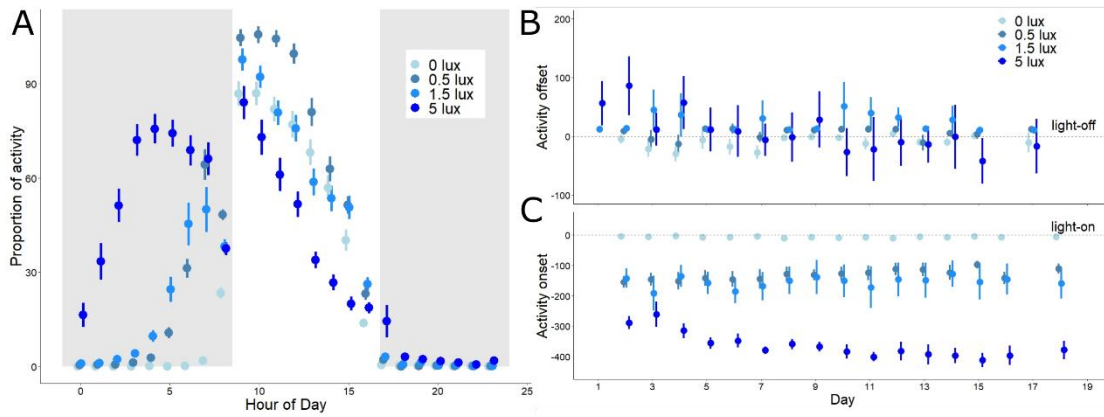
669

670

671

672

673

674

675

Figure 2. Activity timing is affected by intensity of light at night. The proportion of active 2-min intervals in each treatment group per hour of the day is shown in panel (A) (raw mean ± SEM, N = 34). Grey background indicates night-time, white background indicates daytime. On the right, we show daily treatment group data (mean ± SEM), for the timing of (A) evening offset and (B) morning onset of activity (time in min). Activity onset and offset refer to times of lights-on and lights-off, which are shown as the horizonal lines crossing zero in both panels.
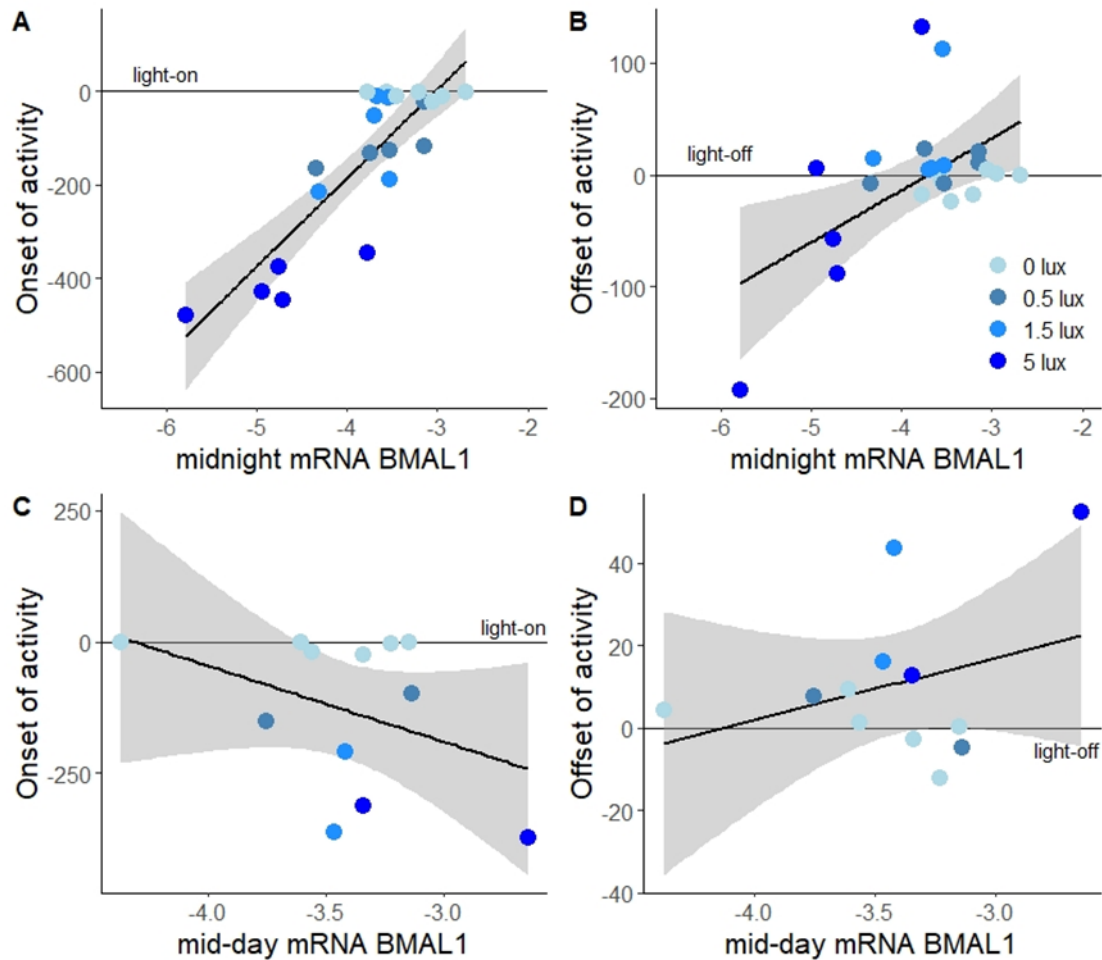
Figure 3. *BMAL1* expression in the hypothalamus predicts the advance of morning activity. mRNA levels of *BMAL1* at midnight correlated with the onset (A) and offset of activity (B), but mid-day levels (C, D) did not. Shown are log-transformed mRNA levels, separated by sampling time (day vs night) and ALAN treatments (blue color gradient). Points represent individual birds (total N = 34), lines and shaded areas represent model fits ± 95% confidence intervals.
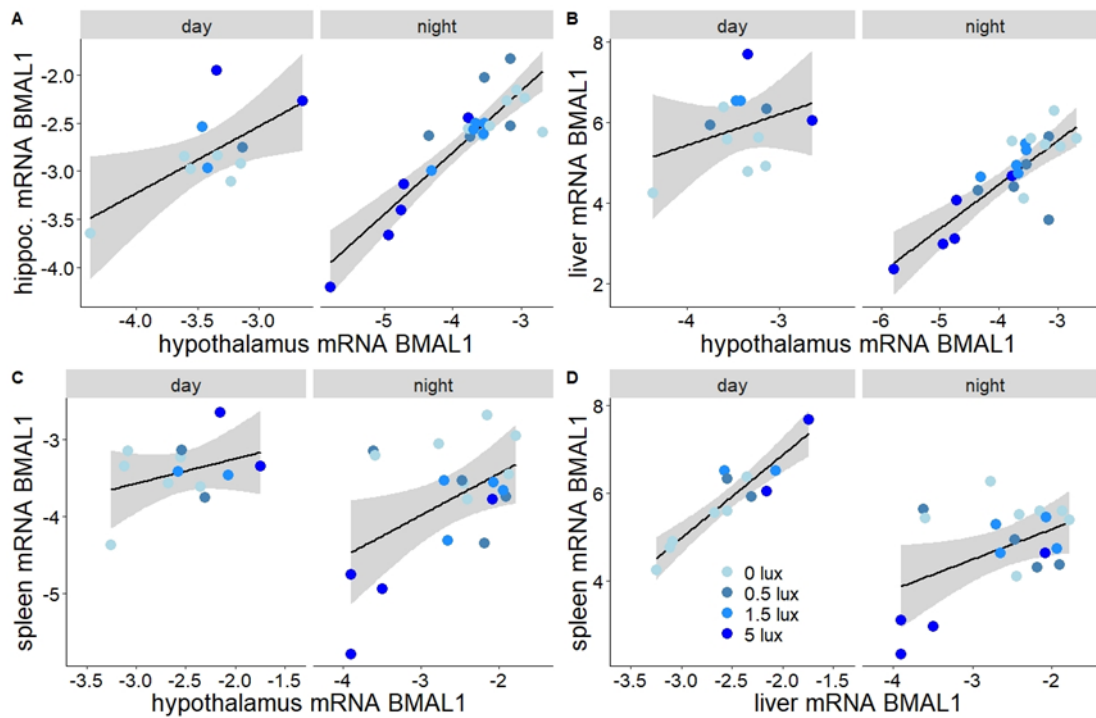
28

Figure 4. ALAN effects on *BMAL1* expression were comparable in different tissues. Correlation of expression patterns of *BMAL1* in different tissues. Shown are log-transformed mRNA levels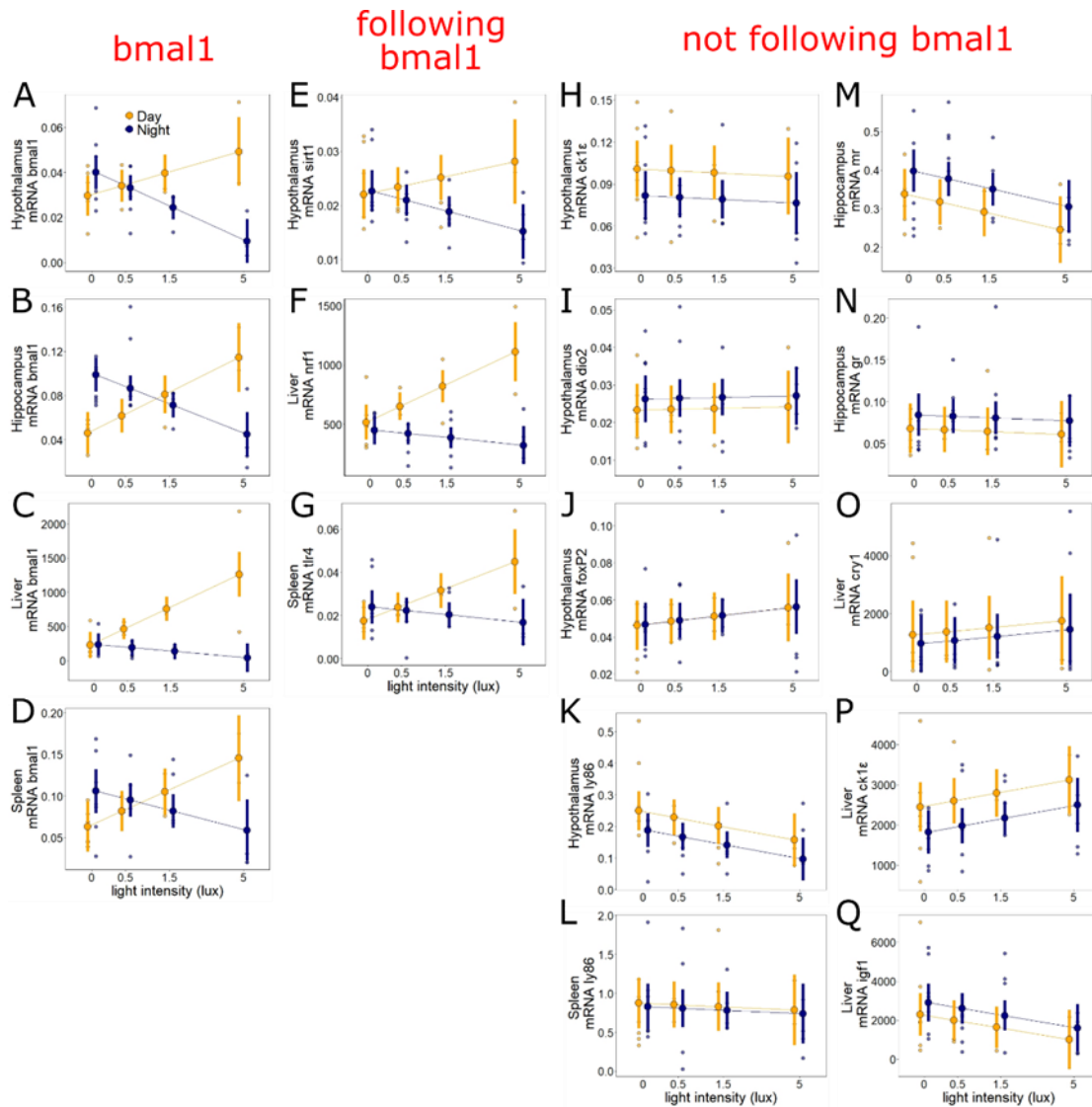, separated by sampling time (day vs night) and ALAN treatments (blue color gradient). Points represent individual birds (N = 34). Lines and shaded areas depict model estimated means ± 95% confidence intervals. Panels show expression levels of hypothalamic *BMAL1* levels in relation to (A) hippocampus, (B) liver and (C) spleen levels, as well as spleen in relation to liver levels (D).

Figure 5. ALAN effects on gene expression are gene-specific. ALAN does not equally affect all physiological systems. ALAN effects on *BMAL1* (A)-(D) were paralleled by those on three additional genes in the hypothalamus (*SIRT1*), liver (*NRF1*) and spleen (*TLR4*) (E)-(G), but not by other genes analyzed across tissues (H)-(Q). Shown are log-transformed mRNA levels, separated by sampling time (mid-day: yellow; midnight: dark blue). Large symbols ± SEM connected by lines represent model estimates, whereas small symbols depict raw data points (N = 34 birds).
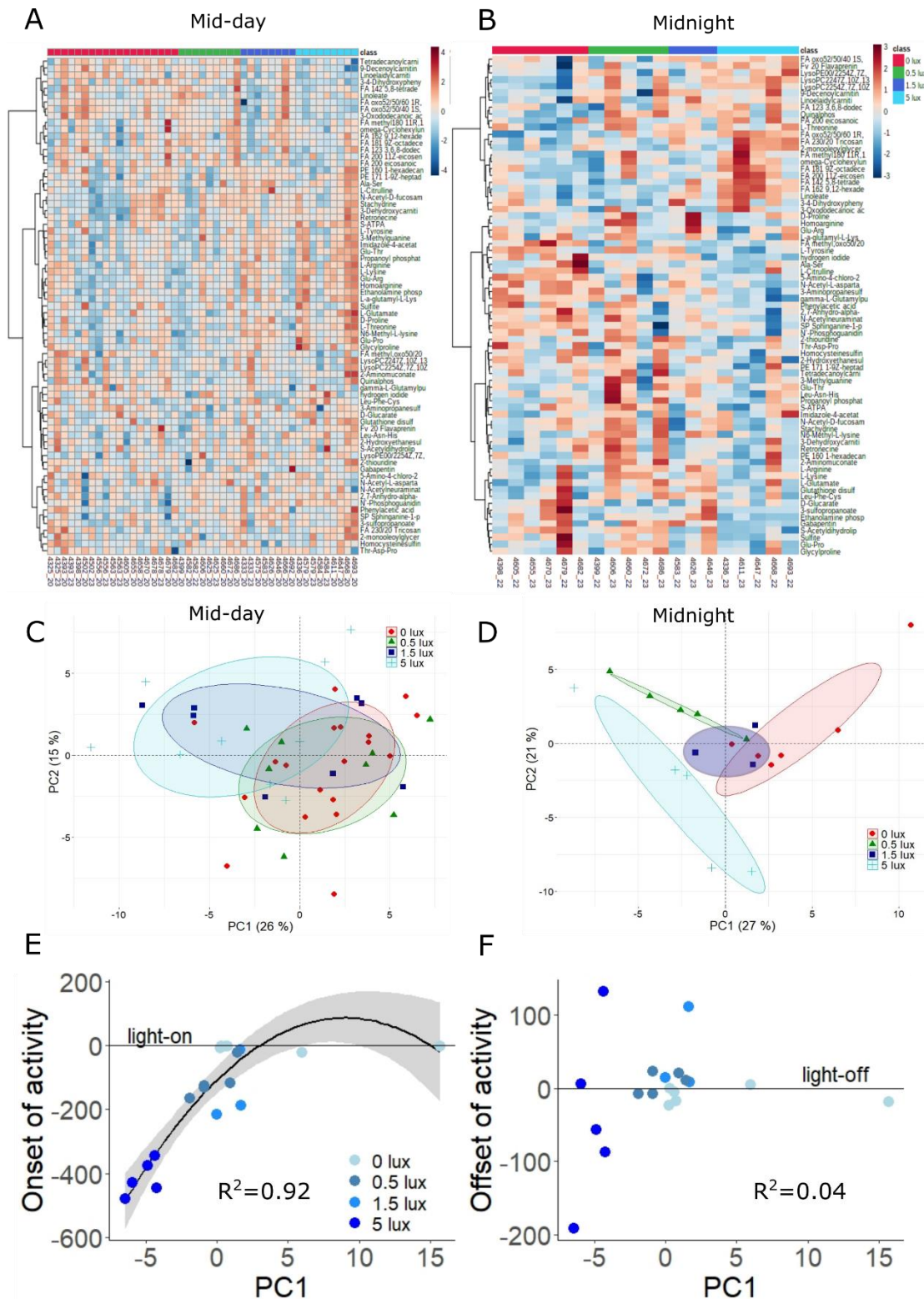
Figure 6. Metabolomics analysis supports ALAN-induced shifts in day-night physiology. The 73 metabolites found to be significantly affected by the interaction of treatment and sampling time (9.6% of all metabolites, interactive dataset) were dissected by means of pathway analysis and principal component analysis. Pathway analysis revealed that the Arginine Biosynthesis pathway was

31

728   particularly enriched in this dataset. Heatmaps show the top-25 metabolites in the interactive dataset

729   at either mid-day (A) or mid-night (B). Principal component analysis showed considerable overlap

730   between ALAN groups at mid-day (C), whereas ALAN treatment effects were mostly visible at midnight,

731   particularly for the 5 lx group (D). In all PCA plots, points represent individual samples, and ellipses

732   contain 80% of samples in a group. The first PC of the night cluster (E) significantly predicted the onset

733   of activity in the morning (D), but not the offset of activity in the evening (F). In (E) and (F) points

734   represent individual birds (N = 19), and lines and shaded areas represent model fits ± 95% confidence

735   intervals.

736

737

738

739

740

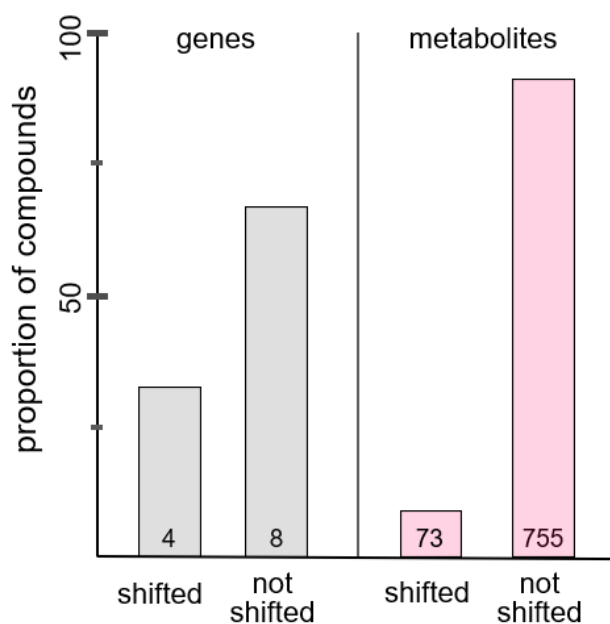741

742

743

744

745

746

747

748

749

750

751

752

753

754

Figure 7. Proportion of shifts in day-night pattern in response to ALAN. Shown are proportions of genes (grey) and metabolites (red) whose levels were, or were not, significantly impacted by the interaction of sampling time and ALAN level.

758

759

760

761

762

763

764

765

766

767

768

769

770

771

772

773

33

774 **Supplementary information for:**

775 Artificial light at night shifts the circadian system but still leads to physiological

776 disruption in a wild bird

777 Davide M. Dominoni[1,2,*], Maaike de Jong[2,3], Kees van Oers[2], Peter O'Shaughnessy[1], Gavin

778 Blackburn[4], Els Atema[2], Christa A. Mateman[2], Pietro B. D'Amelio[5,6,7], Lisa Trost[5], Michelle

779 Bellingham[1], Jessica Clark[1], Marcel E. Visser[2,8], Barbara Helm[1,8]

780

781 * Davide M. Dominoni

782 Email: davide.dominoni@glasgow.ac.uk

783

784 **This PDF file includes:**

785   Detailed methods

786   Supplementary References

787   Figures S1-S8

788   Tables S1-S13

789 **Other supplementary materials for this manuscript include the following:**

790   All datasets and R scripts to reproduce the results of this study are available in
791   Figshare:
792   (https://figshare.com/projects/Artificial_light_at_night_shifts_the_circadian_system_but_stil
793   l_leads_to_physiological_disruption_in_a_wild_bird/88841).

794

795

796

797

798

799

800

801

802

803

804

Supplementary material and methods

Animals and experimental design

805

806

807   We conducted the experiment between February 1 and February 23, 2014, as described elsewhere

808   for these same birds (1). We used 34 adult male great tits that had been used in a previous

809   experiment aimed at assessing the impact of different levels of light intensity at night on daily activity

810   and physiology (2). All birds had been hand-raised and housed at the Netherlands Institute of Ecology

811   (NIOO KNAW), Wageningen, The Netherlands, in indoor-facilities in individual cages (90 × 50 × 40

812   cm). All birds were between 1 and 4 years of age (hatched in 2012 or before), but mean age did not

813   differ significantly between treatment (P = 0.576). Temperature was maintained between 10 and 14

814   °C, and did not vary between day- and night-time. Birds had access to food and water ad libitum. We

815   used dividers between the cages, so that birds could only hear but not see each other, and light from

816   one cage did not influence the light environment in adjacent cages.

817   During the ALAN experiment, birds were kept under fixed natural day-length of 8 hr 15 min

818   light and 15 hr 45 min darkness. Each cage had two separate light sources for day- and night-time

819   illumination. During the day, all birds were exposed to full spectrum daylight by high frequency

820   fluorescent lights emitting ~1000 lux at perch level (Activa 172, Philips, Eindhoven, the Netherlands).

821   For night-time, birds were assigned to different treatment groups that varied in the level of light

822   intensity used (warm white LED light; Philips, Eindhoven, The Netherlands). The spectral composition

823   of this light is shown in Supporting Information Figure S1 of (2), based on an earlier experiment with

824   these birds. In this earlier experiment, the birds were exposed to five levels of ALAN for one month

825   between December 10, 2013 and January 10, 2014 and otherwise kept under dark nights. The

826   experimental setup we used here differed as we used four, and not five experimental levels of ALAN,

827   of which one now was a dark control (0.00, 0.5, 1.5, and 5 lux). The birds in the dark control were

828   derived from the two earlier treatment groups with the lowest light intensity (0.05 and 0.15 lux,

829   respectively), while birds in all other treatments were kept in the same treatment that they were

830   exposed to in the previous experiment. Thus, from the start of our present experiment on February

35

831   1, 2014, the birds were exposed for the entire night to either one out of three nocturnal light

832   intensities measured at perch level in the cages: 0.5 lux (n = 7), 1.5 lux (n = 7), or 5 lux (n = 7), or to

833   dark control conditions (n = 13) (Table S2).

834   The four treatment groups were assigned to one of seven blocks of cages arranged within

835   two experimental rooms. Each block contained all treatment groups, distributed using a Latin

836   Squares design. The birds were kept under these conditions for 3 weeks until culling to collect tissues

837   for morphological, metabolomic and genetic analyses (see more details on this terminal sampling

838   below). On Feb 20th we collected a blood sample (~200 µl) from all birds for metabolomic profiling.

839   The randomly assigned mid-day sampling group was culled on Feb 22nd, and the midnight group

840   during the two subsequent nights (Feb 22nd: 10 birds; Feb 23rd: 12 birds). All experimental procedures

841   were carried out under license NIOO 13.11 of the Animal Experimentation Committee (DEC) of the

842   Royal Netherlands Academy of Arts and Sciences.

843

844   *Locomotor activity*

845   A standard wooden perch and a perch with a micro-switch were fitted into every cage before the

846   start of the experiments. The micro-switch detected perch-hopping and logged the frequency onto a

847   computer. A signal for on (bird on perch) and off (bird not on perch) was recorded every 0.1 s and

848   stored in files as 30 s intervals by software developed by T&M Automation (Leidschendam, The

849   Netherlands). An activity level of either one or zero was obtained for every two minutes, in which a

850   bird was considered active if the micro-switch was triggered once or more times.

851   In total, we examined four different aspects of activity for each bird over a 24-h period with

852   the program Chronoshop 1.1 (by K. Spoelstra). Activity onset (the first time point at which activity is

853   higher than the average) and activity offset (the final time point which activity is higher than the

854   average) were reported relative to when the daylight was switched on and off, respectively. Total

855   activity was defined as the total active minutes within a 24-h cycle (from midnight to midnight), while

856   nocturnal activity was defined as the total number of active minutes during the relative night (lights

857   off until lights on).

858

859   *Tissue preparation*

860   We culled birds under isoflurane anesthesia (Forene, Abbott, Hoofddorp, the Netherlands) at mid-

861   day (±2 hr) on February 22, 2014 or midnight (±2 hr) on February 22 and 23, 2014. Organs were

862   extracted, snap-frozen on dry ice, and stored at −80 ºC within 10 min of capture. The final sample

863   size is shown in Table S2.

864   The whole brain was cut sagittally on a cryostat at − 20 ºC, alternating three sections of 40

865   µm with one section of 60 µm. The 40 µm sections were used to collect tissue for gene expression

866   analysis, thus after being cut they were temporarily stored again at −80 ºC until RNA extraction. The

867   60-µm sections were immediately Nissl-stained and used as reference, to verify histologically that we

868   collected tissue from the regions of interest in the 40 µm sections. From the appearance of the

869   cerebellum in the slides, we collected 120 slices until the disappearance of the cerebellum at the

870   opposite side, using a total of 90 slices for RNA extraction and 30 slices as reference. The

871   hypothalamus and hippocampus in the Nissl-stained series were identified by referencing the

872   Zebrafinch atlas ZEBrA (Oregon Health & Science University, Portland, OR, USA;

873   http://www.zebrafinchatlas.org). To isolate the tissue, for the hypothalamus we sampled one 3 mm

874   of diameter circular tissue punch (Harris Uni-core, Electron Microscopy Sciences, cat#69036) from

875   each section. We used the optic chiasma, medially, the dorsal supraoptic decussation (rostrally, when

876   visible), and the optic tract, laterally, as a reference and punched the medial area immediately dorso-

877   caudal to the optic chiasma (Fig. S1). The collected areas corresponded roughly to the medial basal

878   suprachiasmatic hypothalamus region which is comprised of several nuclei and areas including the

879   suprachiasmatic nuclei (SCN). For the hippocampus, we used forceps to remove the tissue from the

880   medial (enlarged) part of the hippocampus above the lateral ventricle up to the edge of the brain

881   (Fig. S1). Hypothalamic and hippocampal tissues were then immediately added to separate 1.5ml

882   buffer tubes provided by the Qiagen RNeasy micro extraction kit (see below), homogenized and

883   stored at -80 °C until extraction.

884   Whole spleens were homogenized with a ryboliser and added to 1.5 ml RNeasy micro buffer

885   and stored at -80 ºC. For livers, we cut 0.5 g of tissue from each individual liver, homogenized it and

886   added it to 1.5 ml RNeasy micro buffer and stored them at -80 ºC.

887

888   *RNA isolation and cDNA synthesis*

889   RNA isolation and cDNA syntheses was conducted in Glasgow. RNA was extracted using the

890   RNeasy micro extraction kit (Qiagen) following the manufacturer's protocol. RNA quality and quantity

891   were evaluated using a NanoDrop 2000 spectrophotometer (ThermoFisher Scientific). RNA yield was

892   used to adjust the concentration for cDNA synthesis. The working RNA concentration was 25 ng/µl.

893   For each tissue sample, we used 6µl of RNA and reverse transcribed it to generate cDNA using a

894   standard kit following the manufacturer's instructions (Superscript III, Invitrogen). We tested serially

895   diluted cDNA samples for each gene of interest to determine an optimal dilution.

896

897   *Primer design*

898   We made a list of genes known to be involved in circadian and seasonal timing, as well as in

899   metabolism and immune function (Table S1). Similarly, we made a list of reference "housekeeping"

900   genes to allow normalization of the gene expression. Primers were built based on the great tit

901   reference genome build 1.1 (https://www.ncbi.nlm.nih.gov/assembly/GCF_001522545.2) (3) and

902   annotation release 101 (https://www.ncbi.nlm.nih.gov/genome/annotation_euk/Parus_major/101/).

903   Primer design was conducted with Geneious version 10.0.2 (4). Primers were checked against the

904   great tit reference genome using a BLAST search to confirm that primers were specific for the

905   intended target genes. In order to avoid genomic DNA (gDNA) amplification, every primer pair was

906   designed to span an intron of more than 1000 base pairs. Selected primer pairs for the final

907   candidate genes are listed in Table S1.

908

909   *RT-qPCR*

910   Amplification efficiency of each primer pair was determined through quantitative real-time

911   polymerase chain reaction (RT-qPCR). We first analyzed liver samples in Glasgow, measuring

912   fluorescence with a MX3000 cycler 96-well plates (Stratagene). By the time we could analyze brain

913   and spleen samples, logistic issues prevented us to run these assays in Glasgow. Thus, we proceeded

914   with analyses at the NIOO in Wageningen (see below for validation), where fluorescence was

915   measured with the CFX Connect Real-Time PCR Detection System (Bio-Rad Laboratories). In both

916   cases, RT-qPCR was performed by a 5-point standard curve based on a 5-dilution series (1:10, 1:20,

917   1:40, 1:80 and 1:160) of cDNA samples. We included duplicated samples (10 µl) for one transcript on

918   each plate, balancing time points and treatments, using the SYBR Green method (PowerUp SYBR

919   Green Master Mix, ThermoFisher Scientific). At the end of the amplification phase, a melting curve

920   analysis was carried out on the products formed. In each plate, we also included duplicate negative

921   control wells (with RNA instead of cDNA). None of the primer pairs amplified gDNA and the efficiency

922   of the qPCR reactions was always between 95% and 103%.

923   The PCR efficiency and fractional cycle threshold number obtained in Glasgow and

924   Wageningen were used for gene quantification. We used reference gene levels to correct for

925   variation in PCR efficiency and RNA quality between samples. From our list of starting reference

926   genes, we selected two per tissue to correct candidate (target) gene levels. Reference gene

927   expression stability was calculated using the application geNorm (5), from which we identified the

928   best pair of reference genes. Absolute amounts of cDNA were calculated by conversion of the Ct

929   values ($C \times E^{-Ct}$, with $C = 10^{10}$ and $E = 2$) (6). The absolute amounts of the candidate genes were

930   normalized by division by a normalization factor, calculated by taking the geometric mean from the

931   absolute amounts of the reference genes. We thereby obtained relative mRNA transcript levels of

932   the candidate genes.

933

934   *Validation of qPCR data obtained in Glasgow and Wageningen*

935   As quantification of qPCR products might be influenced by the machine used for the analyses, we

936   decided to validate the data produced at the two different laboratories by analysing liver *bmal1*

937   levels in Wageningen, too. Correlation between Glasgow and Wageningen liver data was highly

938   significant (Spearman rho: 0.74, p<0.001).

939

940   *Metabolomics*

941   The 68 plasma samples (34 individuals x 2 time points = 68) were first prepared by the following

942   protocol adjusted for the amount of plasma available (minimally 26 μl): 100 μl of plasma were mixed

943   with chloroform and methanol in a 1:3:1 ratio (chloroform : methanol : sample) on a cooled shaker

944   for one hour and then centrifuged for 3 mins at 13,000g at 4 °C. The resulting supernatant was stored

945   at -80 °C until LC/MC analysis. All samples were analyzed on a Thermo Scientific QExactive Orbitrap

946   mass spectrometer running in positive/negative switching mode. This was connected to a Dionex

947   UltiMate 3000 RSLC system (Thermo Fisher Scientific, Hemel Hempstead, United Kingdom) using a

948   ZIC-pHILIC column (150 mm × 4.6 mm, 5 μm column, Merck Sequant, Gillingham, UK). The column

949   was maintained at 30 °C and samples were eluted with a linear gradient (20 mM ammonium

950   carbonate in water, A and acetonitrile, B) over 46 min at a flow rate of 0.3 mL/min as follows 0 min

951   20% A, 30 min 80% A, 31 min 92% A, 36 min 92% A, 37 min 20% A, 46 min 20% A. The injection

952   volume was 10 μL and samples were maintained at 5 °C prior to injection.

953   Mass spectrometry data were processed using a combination of XCMS 3.2.0 and MZMatch.R

954   1.0–4 (7). Briefly, data were converted from Thermo proprietary raw files to the open format mzXML.

955   Unique signals were extracted using the centwave (8) algorithm and matched across biological

956   replicates based on mass to charge ratio and retention time. These grouped peaks were then filtered

957   based on relative standard deviation and combined into a single file. The combined sets were then

958   filtered on signal to noise score, minimum intensity and minimum detections, leading to the

959   exclusion of four bird samples (final n = 64). The final peak set was then gap-filled and converted to

40

960   text for use with IDEOM v18 (9). IDEOM contained peak data from 5483 compounds. From this

961   dataset, we removed all compounds that IDEOM defined having a confidence lower than 4 (out of

962   10). The majority of these were fragments that did not match to any known standard mass and

963   retention time. Moreover, some metabolites were present twice as two different polarities, in which

964   case only the polarity returning the highest signal was maintained, while the other was removed.

965   Last, metabolites with 0 abundance in more than 10 % of the individuals were also removed. The

966   final dataset contained 755 metabolites.

967

968   *Statistical analysis*

969   All statistical analyses were conducted in R, version 3.63 (10). In all models we included treatment as

970   log-transformed light intensity (adding a constant = 1 to avoid zero returns).

971   To analyze locomotor activity data (i.e. perch-hopping), we first divided the time series of

972   activity into a first phase, before all birds had stabilized their activity timing (defining the day of

973   stabilization as the first day when the mean onset did not differ for more than 1 SEM to the previous

974   and following day), and a stabilized phase thereafter. We first estimated the free-running period of

975   birds during the first 10 days, by calculating the circadian period length using the Lomb-Scargle

976   periodogram analysis implemented in the software Chronoshop (credits to Kamiel Spoelstra). We

977   tested for differences in circadian period length between groups using a Gaussian LM with treatment

978   as explanatory variable.

979   Second, using only the stabilized activity data after day 10, we ran a generalized additive

980   mixed model (GAMM) to test for variation in the proportion of time spent active every hour. Bird ID

981   was included as random factor. We included hour of day, in interaction with treatment, as smoothed

982   terms. The GAMM was run using the function gamm in the package *mgcv* (11).

983   Third, we tested for variation in onset time, offset time, nocturnal activity and total daily

984   activity using separate linear mixed models (LMMs) with ID as random effect, and treatment, day of

41

985   the experiment and their interaction, as well as the quadratic effect of day, as explanatory variables.

986   LMMs were run using the function lmer in the package *lme* (12).

987   To examine variation in relative transcript levels, we ran linear models (LMs) including ALAN

988   treatment, sampling time (two-level factor, day and night), and their interaction as explanatory

989   variables, and mRNA expression levels of the different genes in the different tissues as response

990   variables. We used linear models also to test for individual-level relationships between mRNA levels

991   of the same gene in different tissues, or for the relationship between mRNA levels of different genes

992   withing the same tissue. Moreover, we also used linear models to relate midnight hypothalamic

993   mRNA levels of BMAL1 (explanatory variable) to the mean time of activity onset and offset of each

994   bird. All linear models were run using the function lm in the library *stats* in R.

995   To test for variation in the levels of the individual metabolites identified by the LC-MS, we

996   used all data, including the replicated mid-day samples (total n = 64). Data from the subset of birds

997   sampled both, two days before the culling and during the culling (n = 12; Table S3) were highly

998   correlated (r=0.92 and p<0.001, Fig. S8). We ran independent LMMs for each metabolite, with

999   metabolite levels as response variable (normalized), and treatment, time of day and their interaction

1000   as explanatory variables. ID was always included as random factor. We corrected the p-values of all

1001   these models by the false discovery rate test. Moreover, we ran two principal component analyses

1002   using the function prcomp in the library *stats* in R. For these, we used only the 73 metabolites found

1003   to be significantly affected by the treatment*time interaction. The two PCAs were run on the

1004   individual samples collected at mid-day or midnight, respectively. We then used the first two

1005   principal components (PC1 and PC2) of the midnight based PCA as explanatory variables in two linear

1006   models with onset and offset of activity as response variables, respectively.

1007

1008

1009

1010

Supplementary references

1. D. Dominoni, *et al.*, Dose-response effects of light at night on the reproductive physiology of great tits (Parus major): Integrating morphological analyses with candidate gene expression. *J. Exp. Zool. Part A Ecol. Integr. Physiol.* **2018**, 1–15 (2018).

2. M. de Jong, *et al.*, Dose-dependent responses of avian daily rhythms to artificial light at night. *Physiol. Behav.* **155**, 172–179 (2016).

3. V. N. Laine, *et al.*, Evolutionary signals of selection on cognition from the great tit genome and methylome. *Nat. Commun.* **7**, 10474 (2016).

4. M. Kearse, *et al.*, Geneious Basic: An integrated and extendable desktop software platform for the organization and analysis of sequence data. *Bioinformatics* **28**, 1647–1649 (2012).

5. J. Vandesompele, *et al.*, Accurate normalization of real-time quantitative RT-PCR data by geometric averaging of multiple internal control genes. *Genome Biol.* **3**, research0034.1 (2002).

6. F. Dijk, E. Kraal-Muller, W. Kamphuis, Ischemia-Induced Changes of AMPA-Type Glutamate Receptor Subunit Expression Pattern in the Rat Retina: A Real-Time Quantitative PCR Study. *Investig. Ophthalmol. Vis. Sci.* **45**, 330–341 (2004).

7. R. A. Scheltema, A. Jankevics, R. C. Jansen, M. A. Swertz, R. Breitling, PeakML/mzMatch: A file format, Java library, R library, and tool-chain for mass spectrometry data analysis. *Anal. Chem.* **83**, 2786–2793 (2011).

8. R. Tautenhahn, C. Bottcher, S. Neumann, Highly sensitive feature detection for high resolution LC/MS. *BMC Bioinformatics* **9**, 1–16 (2008).

9. D. J. Creek, A. Jankevics, K. E. V. Burgess, R. Breitling, M. P. Barrett, IDEOM: An Excel interface for analysis of LC-MS-based metabolomics data. *Bioinformatics* **28**, 1048–1049 (2012).

10. R Development Core Team, R: A language and environment for statistical computing. *URL http//www. R-project. org* (2015).

11. ,   CRAN - Package mgcv (December 9, 2020).

12. D. Bates, M. Maechler, B. Bolker, S. Walker, lme4: Linear mixed-effects models using Eigen and S4. *R Packag. version 1.1-12* (2013).

13. B. Helm, M. E. Visser, Heritable circadian period length in a wild bird population. *Proc. R. Soc. B Biol. Sci.* **277**, 3335–3342 (2010).

1047 **Supplementary figures**

1048
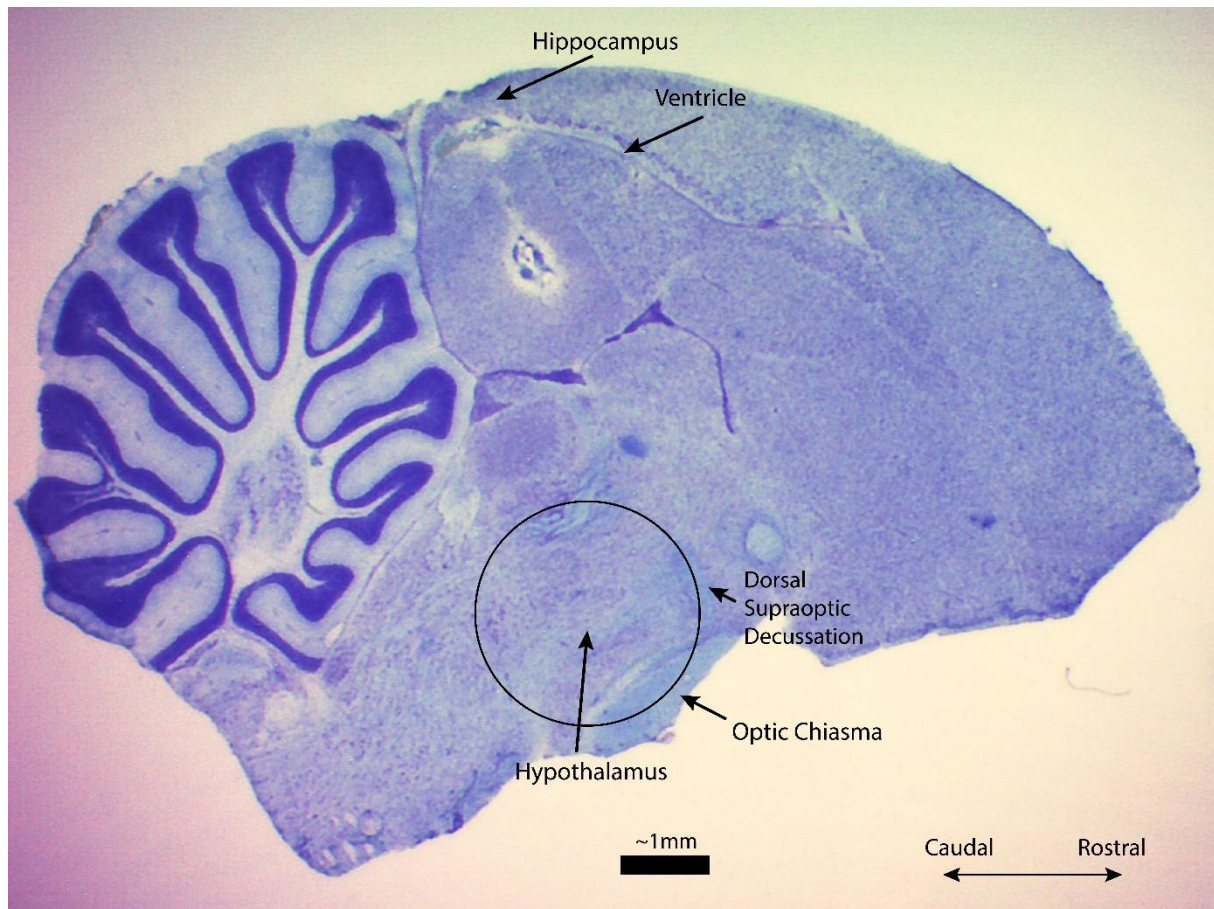
1049

1050 **Figure S1**. Sagittal section of a great tit brain sampled in the experiment. Highlighted are the two
1051 areas used in the analyses: the hypothalamus, sampled via a 3 mm punch in the region just dorso-
1052 caudal of the optic chiasm, caudal of the dorsal supraoptic decussation, and the hippocampus, the
1053 central superior region of the section delimited by the below lateral ventricle.

1054
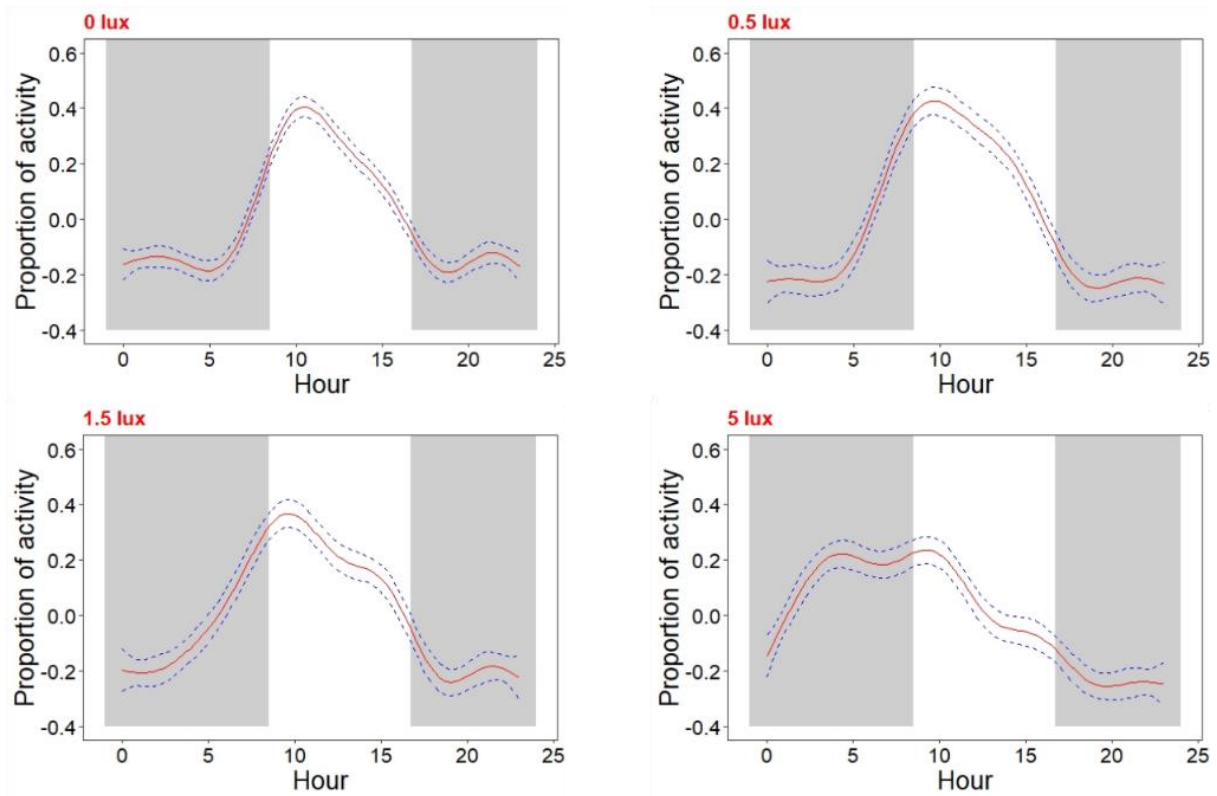
Figure S2. GAMM predictions for each light treatment for the proportion of active 2-min intervals per hour. In each panel, red line depicts predicted mean and blue dashed lines depict 95 % confidence intervals. Grey areas represent night hours, white areas represent daytime.
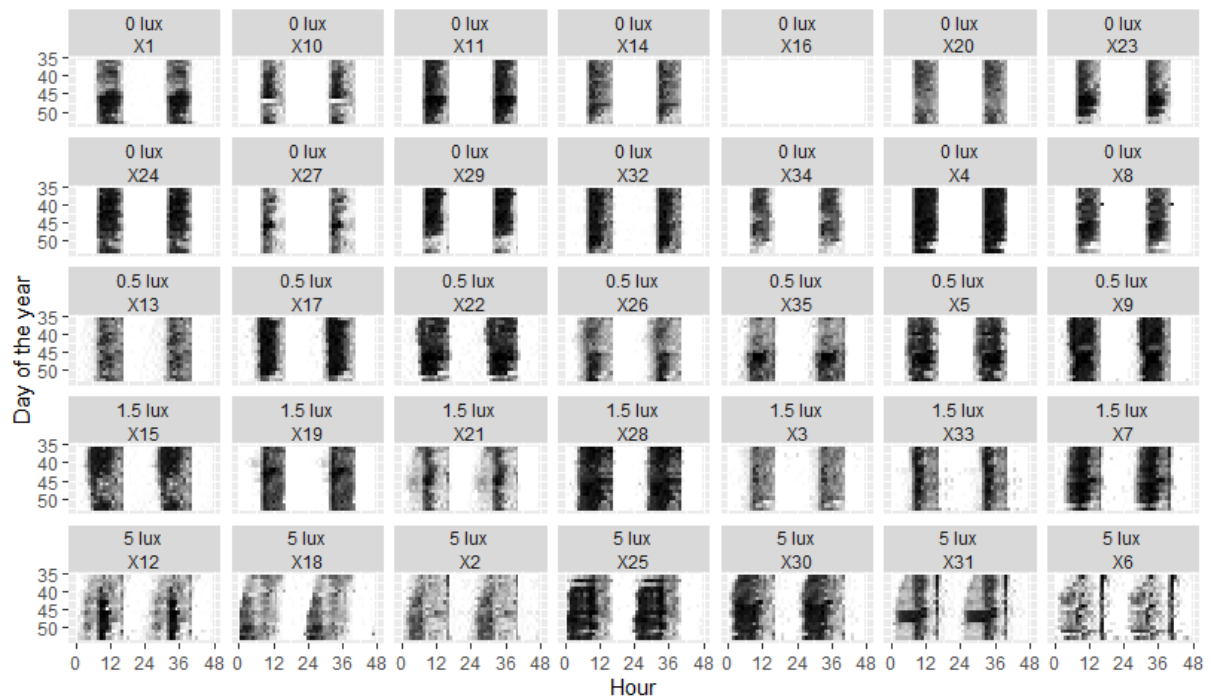
Figure S3. Actograms of all birds used in the experiment. The first two rows represent birds in the 0 lx treatment, the third row birds in the 0.5 lux treatment, the fourth row those in the 1.5 lux treatment, and the last row the birds in the 5 lux treatment. One bird (X16) died before the start of the experiment. Within each plot, rows represent days since the start of the year, and columns the hours of day. The intensity of black represents the amount of activity within each hour bin. Each actogram is double plotted to better visualize free-running rhythms of activity.
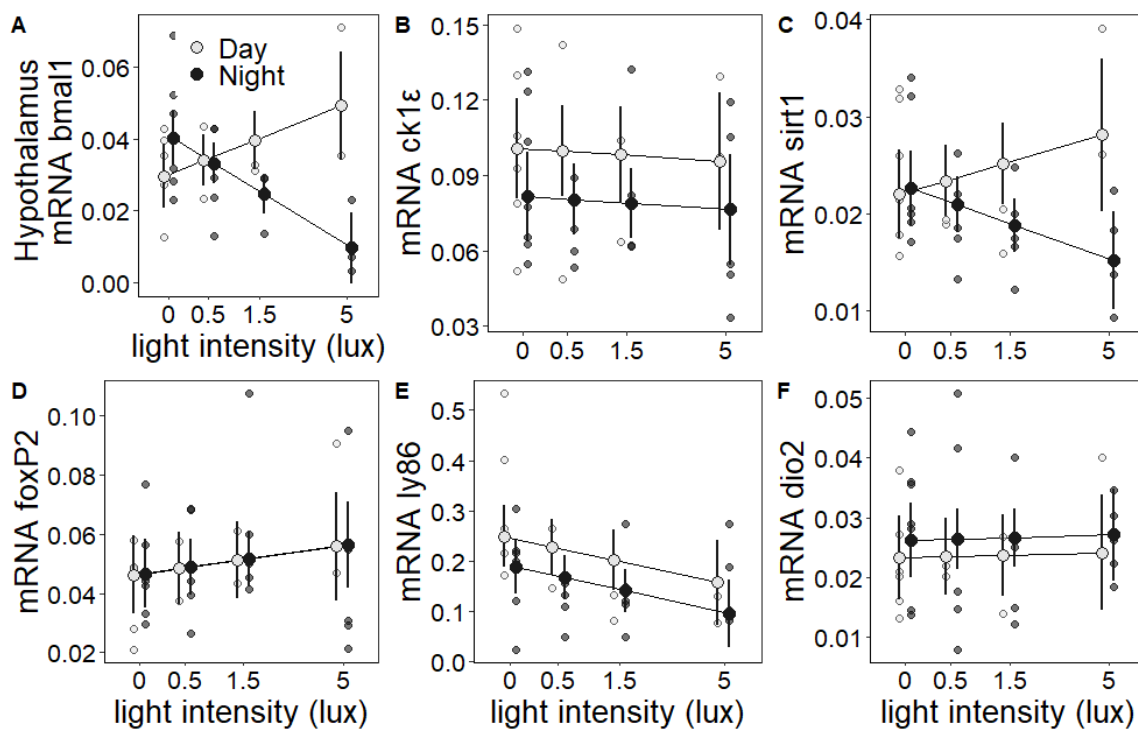
Figure S4. Changes in hypothalamic gene expression in response to ALAN of different intensity measured at mid-day vs. midnight. Large symbols ± SEM connected by lines represent model estimates, whereas small symbols depict raw data points (grey = mid-day, black = midnight).
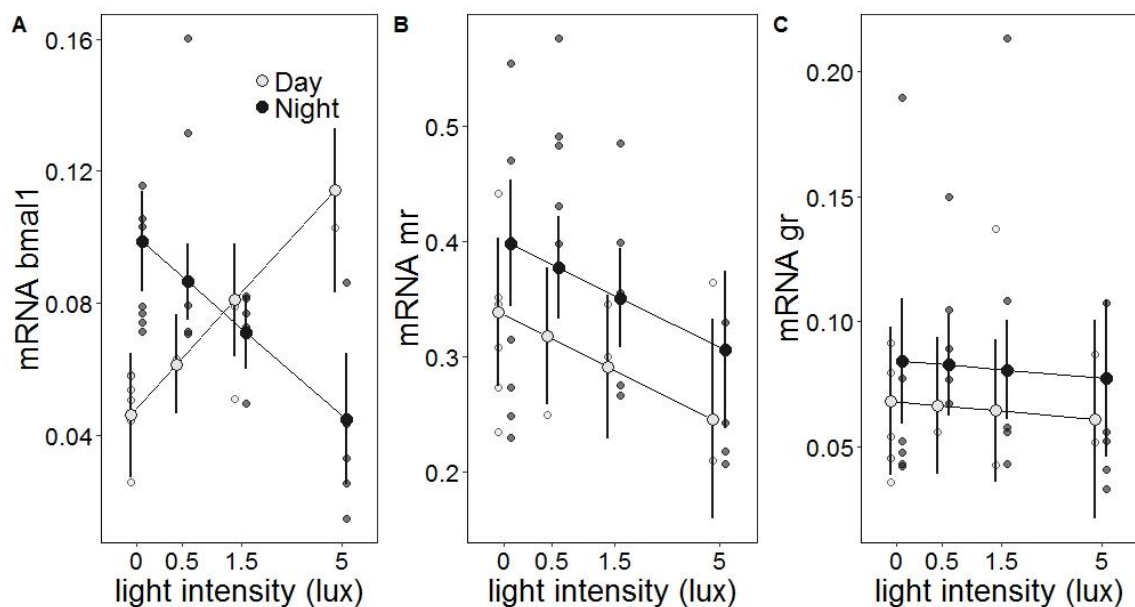
Figure S5. Changes in hippocampal gene expression in response to ALAN of different intensity. Large symbols ± SEM connected by lines represent model estimates, whereas small symbols depict raw data points (grey = mid-day, black = midnight).
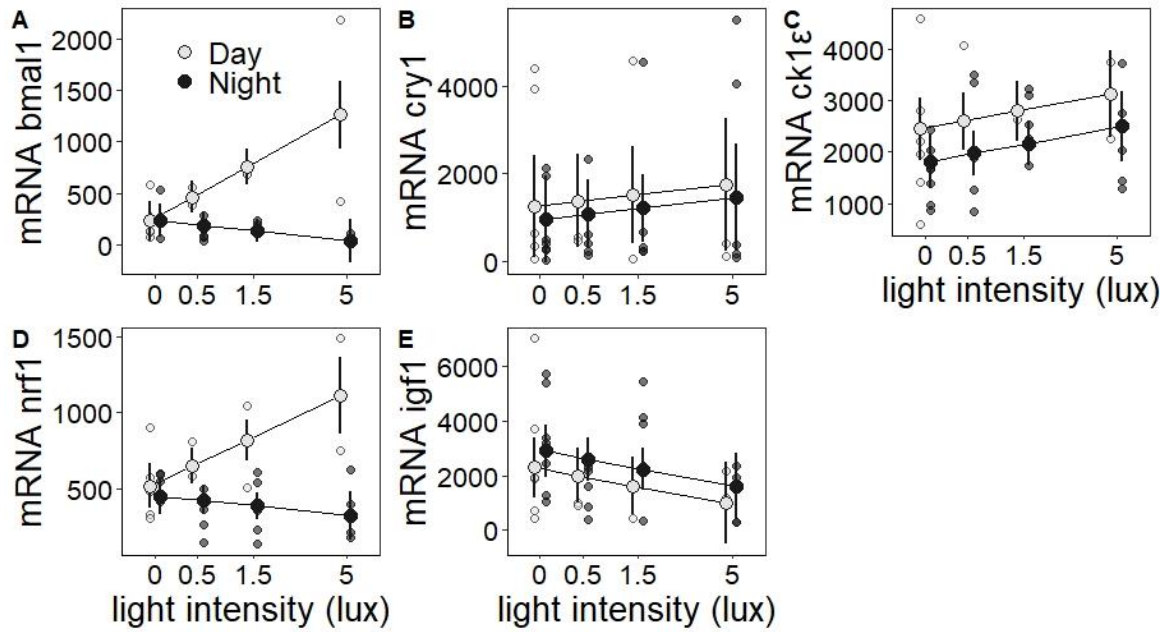
Figure S6. Changes in liver gene expression in response to ALAN of different intensity. One outlier was detected for *CRY1 (panel B)*, however, its exclusion did not qualitatively modify the statistical results. Large symbols ± SEM connected by lines represent model estimates, whereas small symbols depict raw data points (grey = mid-day, black = midnight).
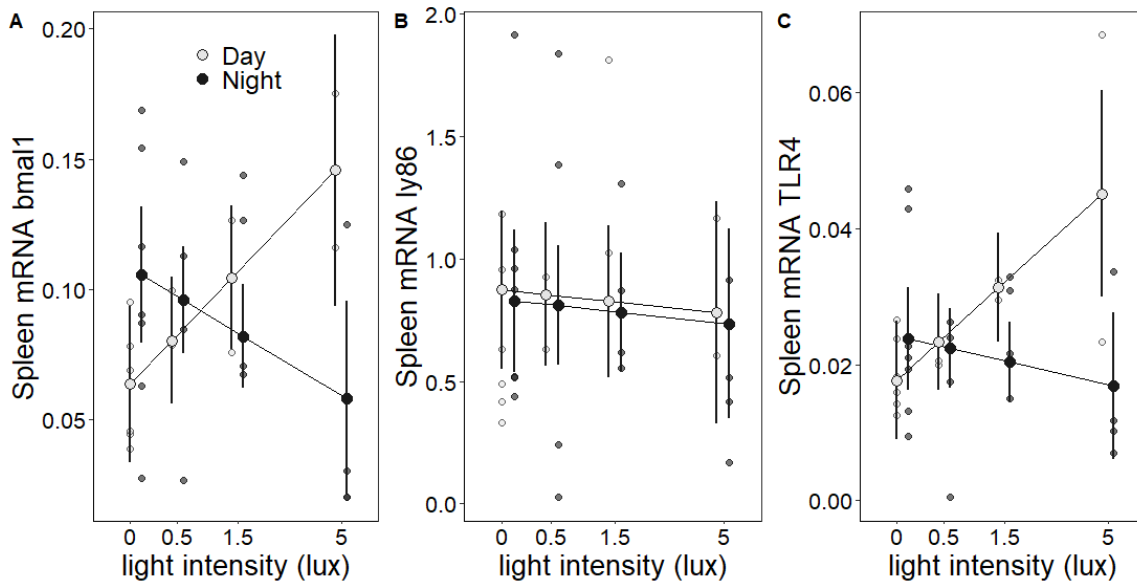
Figure S7. Changes in spleen gene expression in response to ALAN of different intensity. Large symbols ± SEM connected by lines represent model estimates, whereas small symbols depict raw data points (grey = mid-day, black = midnight).
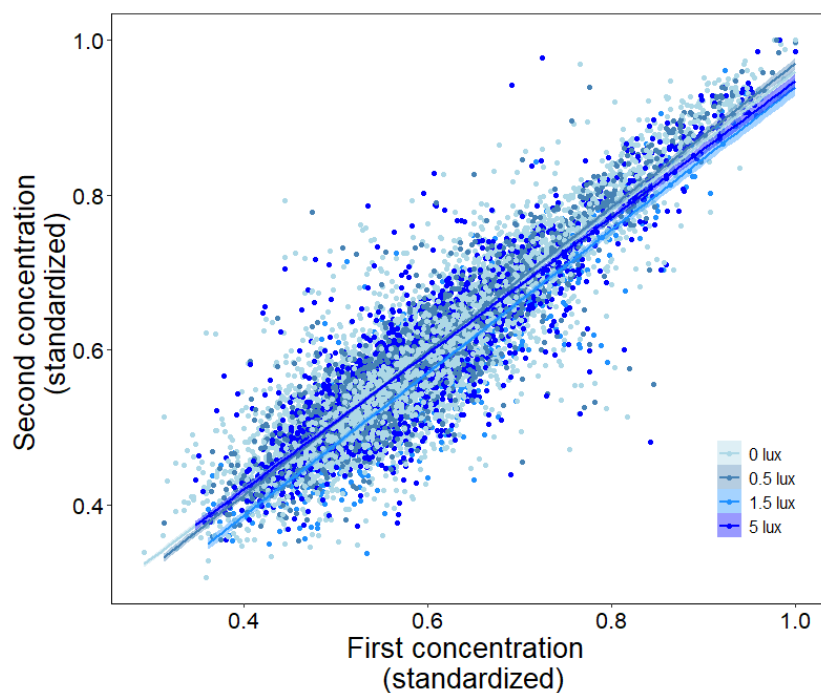
1104

1105

1106 **Figure S8.** Within-individual correlations between standardised metabolite concentration considering
1107 the whole metabolome (892 metabolites). Each point represents one metabolite measured in one
1108 individual two days apart, before the final culling (x-axis) and at the time of culling (y-axis).

1109

Supplementary tables

Table S1. Overview of genes analyzed. Indicated are genes with their full names, a functional note, the tissues where they were measured (Hth=hypothalamus, Hip=hippocampus, Liv=liver, Spl=spleen), and forward and reverse primers for RT-qPCR. Superscripts indicate functional groups. [a] clock genes and modulators; [b] seasonal regulators; [c] metabolic genes; [d] immune genes; [e] endocrine genes; [f] reference genes.

Gene	Full name	Functional note	Hth	Hip	Liv	Spl	Forward	Reverse
[a] *bmal1 (arntl)*	Brain and Muscle ARNT-Like1	core clock gene	yes	yes	yes	yes	cgcttcgtggtgctacaaac	ccatctgctgccctgagaat
[a] *cry1*	Cryptochrome Circadian Regulator 1	core clock gene			yes		tcaccatttagccccggcatgc	gaaagaaggaactacaggacagccacatc
[a] *ck1ε (CSNK1E)*	Casein kinase I isoform epsilon	posttranslational modulator of clock proteins (PER)	yes		yes		cattaagtggtgtggagcag	aaatttgcgggaacagaagt
[b] *dio2*	Type II iodothyronine deiodinase	converts thyroxine (T4) to bioactive thyroid hormone triiodothyronine (T3)	yes				tccacacttgccaccaacat	caaactgggaggagaagccc
[b] *foxP2*	Forkhead box protein P2	transcription factor involved in vocal learning and plasticity	yes				aaaggagcagtatggacagt	agctggtgggtatgtttttc
[c] *sirt1*	Sirtuin 1	enzyme deacetylating transcription factors (clock-, stress-, ageing- linked)	yes				gtcacaagttcatcgctttg	atcctttggattcctgcaac
[c] *nrf1*	Nuclear Respiratory Factor 1	key nuclear transcription factor of involved in mitochondrial activity			yes		gggccacgctggatgagtaca	gccagcgccgattccagat
[d] *ly86 (MD1)*	Lymphocyte antigen 86	regulates T cell activation and cytokine production	yes			yes	gaccattgtgctgatattgcaaccc	agcttatcatgacccggccca
[d] *tlr4*	Toll-like receptor 4	Pattern recognition factor, innate immune system activation				yes	cacctccacaccttggatatt	tcgaaggtcaggagcttattg
[e] *nr3c1 (gr)*	Nuclear receptor subfamily 3, group C, member 1	glucocorticoid receptor		yes			attggctccgctgggaacg	aggcctcgtcagagcacacca
[e] *nr3c2 (mr)*	Nuclear receptor subfamily 3, group C, member 2	mineralocorticoid receptor		yes			tgtgtctgtcatcgtttgccttgag	cggacgaactgcaggctgatct
[e] *igf1*	Insulin-like growth factor 1	hormone linked to mitochondrial biogenesis, respiration and ageing			yes		ttgctgctggcccagaaacac	cacaactctggaagcagcattcatcc
[f] *RPL13*	ribosomal protein L13	component of ribosome	yes	yes	yes		tactccttcagcctctgcac	acaagaagtttgcccggact
[f] *RPL19*	ribosomal protein L19	component of ribosome	yes			yes	ctgcggcaagaagaaggtgt	tcagcccatccttgatcagc
[f] *SDHA*	Succinate Dehydrogenase Complex Flavoprotein Subunit	mitochondrial respiratory chain		yes	yes	yes	gggcaataactccacggcat	ttgtatggcaggtctctacga
[f] *PMM1*	Phosphomannomutase	glycosylation			yes		caccccagaggagcgaatcga	tcgagcacattgaggcagtagcg
[f] *TBP*	TATA-binding protein	general transcription factor			yes		aaaactattgcacttcgtgcccga	gaatatcagtgcagtggtacgtggttctct

1   **Table S2.** Sample sizes for treatment and time of sampling used in the gene expression analyses.

Treatment	Day	Night
0 lux	6	7
0.5 lux	2	5
1.5 lux	2	5
5 lux	2	5

2

3

4

5   **Table S3.** Sample sizes for treatment and time of sampling used for the metabolomics analysis.
6   All birds were sampled at mid-day two days before the final culling, on Feb 20th. Birds were then
7   re-sampled at mid-day or midnight during the culling. Metabolomics data from 64 individual bird
8   samples (4 samples were excluded due to low signal in the LC-MS data) were used in our
9   analyses. For a subset of birds (n = 12, the sum of all birds sampled at mid-day during culling),
10   we have two mid-day samples which we used to examine within-individual correlation of
11   metabolite levels (see Fig. S8 for these results).

Treatment	Pre-culling samples (Feb 20th 2014)	Culling samples (Feb 22nd & 23rd 2014)	
	Day	Day	Night
0 lux	13	6	6
0.5 lux	7	2	5
1.5 lux	6	2	3
5 lux	7	2	5

12

13

14

15

16

17

18

19

20

21   **Table S4.** Results of generalized additive mixed model (GAMM) testing for variation in the
22   proportion of 2-min intervals spent active per hour of day, depending on night light intensity.
23   Treatment was included as linear predictor. Hour of day was included as smoothed predictor,
24   and we included four smoothed terms referring to the four treatments. Plots for these
25   smoothed terms can be seen in Fig. 2 of the main text.

26

Parametric coefficients				
Predictor	*Estimate*	*Std. Error*	*t value*	*p value*
Intercept	0.18	0.01	14.51	< 0.001
Treatment	0.02	0.01	3.18	**0.001**
Significance of smooth terms:				
Predictor	*F*	*p value*		
s(Hour of Day)*Treatment 0 lux	177.38	**<0.001**		
s(Hour of Day)*Treatment 0.5 lux	141.02	**<0.001**		
s(Hour of Day)*Treatment 1.5 lux	95.86	**<0.001**		
s(Hour of Day)*Treatment 5 lux	81.13	**<0.001**		

27

28

29 **Table S5.** Results of Gaussian linear mixed models testing for variation in activity levels
30 depending on night light intensity, day of the experiment and their interaction. The day of the
31 experiment was also coded as a quadratic term for testing non-linear changes in activity traits
32 over the course of the experiment after the initial exposure to ALAN. The error structure used in
33 each model is specified in brackets.

34

Onset of activity

predictor	estimate	std.error	t value	p value
Intercept	-134.7	10.4	-12.92	<0.001
Day	-23.7	9.8	-2.41	**0.017**
Treatment	-124.9	10.4	-11.96	**<0.001**
Day^2	19	9.3	2.04	**0.042**
Treatment*Day	-34.6	9.9	-3.52	**<0.001**
Treatment*Day^2	19.4	9.3	2.08	**0.038**

Offset of activity

predictor	estimate	std.error	t value	p value
Intercept	4.2	7.5	0.56	0.578
Day	-8	7.6	-1.06	0.289
Treatment	8.4	7.5	1.12	0.271
Day^2	4.5	7.6	0.59	0.556
Treatment*Day	-10.9	1.8	-6.15	**<0.001**

Nocturnal activity

predictor	estimate	std.error	t value	p value
Intercept	-1.7	0.1	-12.1	**<0.001**
Day	0.1	0.1	0.51	**<0.001**
Treatment	1.1	0.1	8.83	**<0.001**

Total 24h activity

predictor	estimate	std.error	t value	p value
Intercept	377.7	17.3	21.78	**<0.001**
Day	41.9	10.8	3.87	**<0.001**
Treatment	32.8	17.4	1.89	0.068
Day^2	-30.9	10.8	-2.86	**0.004**
Treatment*Day	14.6	2.5	5.77	**<0.001**

35

36

37

38 **Table S6.** Estimated period length (tau) of Great tits exposed to ALAN until activity patterns
39 stabilized. Shown are estimated means from a Gaussian LM and outcomes of Tukey post-hoc
40 testing for differences in tau through pair-wise contrasts of treatment groups. Tau was
41 estimated via Lomb-Scargle periodogram analysis implemented in the software Chronoshop
42 (courtesy of Kamiel Spoelstra), using only the first 10 days of activity data. During this phase
43 shifting interval, period lengths in the 5 lx group were similar to the reported free-running
44 period length of this species (13).

45

Estimated means			
treatment	*estimated mean (mins)*	*lower 95 % CI*	*upper 95% CI*
0 lux	23.95	23.88	24.01
0.5 lux	23.89	23.80	23.97
1.5 lux	23.85	23.76	23.94
5 lux	23.59	23.50	23.68
Post-hoc test			
contrast	*estimated difference (mins)*	*std.error*	*P value*
0 lux - 0.5 lux	3.8	3.2	0.646
0 lux - 1.5 lux	6.1	3.2	0.254
0 lux - 5 lux	21.5	3.2	**<0.001**
0.5 lux - 1.5 lux	2.3	3.7	0.924
0.5 lux - 5 lux	17.7	3.7	**<0.001**
1.5 lux - 5 lux	15.4	3.7	**0.001**

46

47

48

49

50

51

52

53

54

55

56

57

58   **Table S7.** Results of linear models (Gaussian error structure) testing for variation in mRNA levels
59   of six different genes in the hypothalamus. Estimates for the predictor sampling time refer to
60   midnight values, while mid-day values are the reference level.

HYPOTHALAMUS GENE EXPRESSION

bmal1

predictor	estimate	std.error	t value	p value
Intercept	0.03	0.004	6.8	<0.001
Treatment	0.011	0.005	2.1	**0.044**
Time	0.01	0.006	1.84	0.076
Treatment*Time	-0.028	0.006	-4.37	**<0.001**

ck1ε

predictor	estimate	std.error	t value	p value
Intercept	0.101	0.01	10.32	**<0.001**
Treatment	-0.003	0.008	-0.38	0.709
Time	-0.019	0.011	-1.72	0.095

sirt1

predictor	estimate	std.error	t value	p value
Intercept	0.022	0.002	9.83	<0.001
Treatment	0.003	0.003	1.26	0.216
Time	0.001	0.003	0.22	0.831
Treatment*Time	-0.008	0.003	-2.29	**0.029**

dio2

predictor	estimate	std.error	t value	p value
Intercept	0.023	0.003	6.75	<0.001
Treatment	0	0.003	0.17	0.866
Time	0.003	0.004	0.76	0.455

foxp2

predictor	estimate	std.error	t value	p value
Intercept	0.046	0.007	7.07	<0.001
Treatment	0.005	0.005	1.02	0.317
Time	0	0.007	0.05	0.958

ly86

predictor	estimate	std.error	t value	p value
Intercept	0.249	0.03	8.29	<0.001
Treatment	-0.051	0.024	-2.12	**0.042**
Time	-0.061	0.034	-1.79	0.083

61   **Table S8.** Results of linear models (Gaussian error structure) testing for variation in mRNA levels
62   of three different genes in the hippocampus. Estimates for the predictor sampling time refer to
63   midnight values, while mid-day values are the reference level.

64

HIPPOCAMPUS GENE EXPRESSION

bmal1

predictor	estimate	std.error	t value	p value
Intercept	0.046	0.009	5.03	<0.001
Treatment	0.038	0.011	3.59	**0.001**
Time	0.053	0.012	4.45	**<0.001**
Treatment*Time	-0.068	0.013	-5.22	**<0.001**

mineralocorticoid receptor

predictor	estimate	std.error	t value	p value
Intercept	0.338	0.032	10.69	<0.001
Treatment	-0.052	0.025	-2.11	**0.044**
Time	0.06	0.036	1.67	0.105

glucocorticoid receptor

predictor	estimate	std.error	t value	p value
Intercept	0.068	0.015	4.67	<0.001
Treatment	-0.004	0.011	-0.35	0.728
Time	0.016	0.016	0.99	0.329

65

66

67

68

69

70

71

72

73

74

75

76

77　**Table S9.** Relationships between *BMAL1* mRNA levels in different tissues. Shown are results of
78　Gaussian linear models testing for the relationship between mRNA levels (all log-transformed) in
79　two tissues per model, while controlling for sampling time and treatment, which were included
80　as covariates in all models.

81

bmal1 **hippocampus ~** *bmal1* **hypothalamus**				
Predictor	*Estimate*	*Std. Error*	*t value*	*p value*
Intercept	-0.44	0.30	-1.50	0.145
bmal1 hypothalamus	0.71	0.09	8.02	**< 0.001**
Time	0.40	0.11	3.72	0.001
Treatment	0.04	0.03	1.44	0.160
bmal1 **liver ~** *bmal1* **hypothalamus**				
Predictor	*Estimate*	*Std. Error*	*t value*	*p value*
Intercept	9.62	0.77	12.57	< 0.001
bmal1 hypothalamus	1.11	0.23	4.89	**< 0.001**
Time	-0.80	0.27	-2.97	0.006
Treatment	0.04	0.08	0.58	0.567
bmal1 **spleen ~** *bmal1* **hypothalamus**				
Predictor	*Estimate*	*Std. Error*	*t value*	*p value*
Intercept	-2.17	0.43	-5.10	< 0.001
bmal1 hypothalamus	0.43	0.16	2.72	**0.011**
Time	-0.28	0.20	-1.41	0.170
Treatment	-0.13	0.05	-2.46	0.021
bmal1 **spleen ~** *bmal1* **liver**				
Predictor	*Estimate*	*Std. Error*	*t value*	*p value*
Intercept	-4.71	0.65	-7.30	< 0.001
bmal1 liver	0.37	0.10	3.59	**0.001**
Time	0.32	0.23	1.42	0.166
Treatment	0.00	0.05	0.02	0.987

82

83

84

85 **Table S10.** Results of linear models (Gaussian error structure) testing for variation in mRNA
86 levels of four different genes in the liver. Estimates for the predictor sampling time refer to
87 midnight values, while mid-day values are the reference level.

88

LIVER GENE EXPRESSION

bmal1

predictor	estimate	std.error	t value	p value
Intercept	228.703	94.065	2.43	0.021
Treatment	576.357	112.237	5.14	**<0.001**
Time	4.893	122.818	0.04	0.968
Treatment*Time	-684.509	138.231	-4.95	**<0.001**

ck1ε

predictor	estimate	std.error	t value	p value
Intercept	2446.672	300.406	8.14	<0.001
Treatment	376.241	242.042	1.55	0.131
Time	-625.039	342.306	-1.83	0.078

nrf1

predictor	estimate	std.error	t value	p value
Intercept	516.546	71.402	7.23	<0.001
Treatment	330.961	85.196	3.88	**0.001**
Time	-65.376	93.228	-0.7	0.489
Treatment*Time	-402.217	104.928	-3.83	**0.001**

igf1

predictor	estimate	std.error	t value	p value
Intercept	2289.529	541.793	4.23	<0.001
Treatment	-720.868	436.532	-1.65	0.109
Time	604.69	617.361	0.98	0.335

89

90

91

92

93

94

95

96 **Table S11.** Results of linear models (Gaussian error structure) testing for variation in mRNA
97 levels of three different genes in the spleen. Estimates for the predictor sampling time refer to
98 midnight values, while mid-day values are the reference level.

99

SPLEEN GENE EXPRESSION

bmal1

predictor	estimate	std.error	t value	p value
Intercept	0.063	0.015	4.3	0
Treatment	0.046	0.018	2.61	**0.015**
Time	0.043	0.019	2.19	**0.037**
Treatment*Time	-0.072	0.022	-3.25	**0.003**

ly86

predictor	estimate	std.error	t value	p value
Intercept	0.873	0.158	5.52	0
Treatment	-0.049	0.132	-0.37	0.711
Time	-0.045	0.183	-0.25	0.806

tlr4

predictor	estimate	std.error	t value	p value
Intercept	0.018	0.004	4.09	0
Treatment	0.015	0.005	2.98	**0.006**
Time	0.006	0.006	1.12	0.272
Treatment*Time	-0.019	0.006	-2.97	**0.006**

100

101

102

103

104

105

106

107

108

109

110 **Table S12.** List of 29 metabolites significantly affected by the linear effect of treatment, as
111 tested via individuals LMMs run on all 755 identified metabolites. P-values were corrected using
112 a false discovery rate of 0.05.

metabolite	F value	p value	p (fdr)
β-ketophosphonate	12	0.002	0.013
[FA] O-Palmitoyl-R-carnitine	7.7	0.007	0.035
[PC (20:0)] 1-eicosanoyl-sn-glycero-3-phosphocholine	11.6	0.002	0.012
[PC acetyl(17:2)] 1-heptadecyl-2-acetyl-sn-glycero-3-phosphocholine	10.4	0.003	0.017
1,2-dioctanoyl-1-amino-2,3-propanediol	11	0.002	0.014
3-4-DihydroxyphenylglycolO-sulfate	7.4	0.009	0.039
4-Pyridoxate	8.7	0.006	0.03
Ala-Asp-Pro	8.4	0.007	0.033
Anandamide	12.8	0.001	0.005
D-Glucuronate	12.8	0.001	0.008
D-Ornithine	7.4	0.008	0.038
dimethylsulfonio-2-hydroxybutyrate	7.7	0.01	0.042
gamma-L-Glutamylputrescine	8.7	0.004	0.024
Glu-Arg	9.4	0.003	0.018
Glu-Thr	7.7	0.007	0.034
Glyceraldehyde	7.1	0.01	0.042
Hypotaurine	11.7	0.002	0.011
Imidazole-4-acetate	10.9	0.002	0.01
L-a-glutamyl-L-Lysine	9.6	0.003	0.017
L-Aspartate	7.3	0.009	0.04
L-Cysteinylglycinedisulfide	6.8	0.009	0.041
Leucyl-leucine	6.9	0.011	0.046
LysoPE(0:0/22:0)	8.8	0.006	0.028
Ne,Ne dimethyllysine	7.3	0.009	0.039
Protoporphyrin	7.1	0.01	0.042
Stearoylcarnitine	9.3	0.003	0.019
Taxa-4(20),11(12)-dien-5alpha-yl acetate	8.9	0.004	0.022
Tetradecanoylcarnitine	12.2	0.001	0.01
Xylitol	6.9	0.011	0.046

113

114 **Table S13.** List of 73 metabolites significantly affected by the interaction of treatment and
115 sampling time, as tested via individuals LMMs run on all 755 identified metabolites. P-values were
116 corrected using a false discovery rate of 0.05.

metabolite	F value	p value	p (fdr)
(S)-ATPA	7.9	0.007	0.027
[FA (12:3)] 3,6,8-dodecatrien-1-ol	4.5	0.039	0.047
[FA (14:2)] 5,8-tetradecadienoic acid	4.5	0.04	0.047
[FA (16:2)] 9,12-hexadecadienoic acid	5.4	0.025	0.044
[FA (18:1)] 9Z-octadecenoic acid	6.2	0.017	0.041
[FA (20:0)] 11Z-eicosenoic acid	9.8	0.003	0.026
[FA (20:0)] eicosanoic acid	4.6	0.037	0.047
[FA (23:0/2:0)] Tricosanedioic acid	8.1	0.007	0.027
[FA methyl(18:0)] 11R,12S-methylene-octadecanoic acid	5.8	0.021	0.042
[FA methyl,oxo(5:0/2:0)] 2-methylene-4-oxo-pentanedioic acid	5	0.029	0.046
[FA oxo(5:2/5:0/4:0)] (1S,2S)-3-oxo-2-pentyl-cyclopentanebutanoic acid	4.8	0.034	0.047
[FA oxo(5:2/5:0/6:0)] (1R,2R)-3-oxo-2-pentyl-cyclopentanehexanoic acid	8.2	0.007	0.027
[Fv (2:0)] Flavaprenin 7,4'-diglucoside	10.4	0.002	0.024
[PE (16:0)] 1-hexadecanoyl-sn-glycero-3-phosphoethanolamine	4.6	0.037	0.047
[PE (17:1)] 1-(9Z-heptadecenoyl)-sn-glycero-3-phosphoethanolamine	4.2	0.044	0.047
[SP] Sphinganine-1-phosphate	7.6	0.008	0.03
2-Aminomuconate	9.1	0.005	0.027
2-Hydroxyethanesulfonate	5.4	0.024	0.043
2-monooleoylglycerol	5.9	0.019	0.042
2-thiouridine	6.6	0.012	0.038
2,7-Anhydro-alpha-N-acetylneuraminic acid	6.6	0.013	0.039
3-4-DihydroxyphenylglycolO-sulfate	4.7	0.036	0.047
3-Aminopropanesulfonate	11.5	0.001	0.022
3-Dehydroxycarnitine	6.5	0.015	0.041
3-Methylguanine	4.3	0.045	0.047
3-Oxododecanoic acid	5.1	0.029	0.046
3-sulfopropanoate	4.1	0.048	0.048
5-Amino-4-chloro-2-(2,3-dihydroxyphenyl)-3(2H)-pyridazinone	5.5	0.022	0.043
9-Decenoylcarnitine	8.2	0.007	0.027
Ala-Ser	6.2	0.016	0.041
D-Glucarate	4.3	0.043	0.047
D-Proline	4.7	0.037	0.047
Ethanolamine phosphate	8	0.006	0.027
Gabapentin	5.7	0.021	0.042
gamma-L-Glutamylputrescine	13	0.001	0.022
Glu-Arg	5.5	0.023	0.043
Glu-Pro	11.3	0.002	0.022
Glu-Thr	4.1	0.049	0.049

Glutathione disulfide	4.1	0.047	0.048
Glycylproline	4.5	0.04	0.047
Homoarginine	4.6	0.038	0.047
Homocysteinesulfinicacid	4.7	0.034	0.047
hydrogen iodide	4.5	0.038	0.047
Imidazole-4-acetate	4.6	0.035	0.047
L-a-glutamyl-L-Lysine	6	0.017	0.041
L-Arginine	5.4	0.025	0.044
L-Citrulline	4.5	0.04	0.047
L-Glutamate	5.1	0.027	0.045
L-Lysine	7	0.012	0.038
L-Threonine	5.7	0.019	0.042
L-Tyrosine	12.6	0.001	0.022
Leu-Asn-His	6.3	0.016	0.041
Leu-Phe-Cys	4.3	0.043	0.047
Linoelaidylcarnitine	4.1	0.047	0.048
Linoleate	8.9	0.005	0.027
LysoPC(22:4(7Z,10Z,13Z,16Z))	4.6	0.038	0.047
LysoPC(22:5(4Z,7Z,10Z,13Z,16Z))	10.7	0.002	0.022
LysoPE(0:0/22:5(4Z,7Z,10Z,13Z,16Z))	4.3	0.042	0.047
N'-Phosphoguanidinoethyl methyl phosphate	7.9	0.007	0.027
N-Acetyl-D-fucosamine	9.1	0.005	0.027
N-Acetyl-L-aspartate	6.2	0.015	0.041
N-Acetylneuraminate	7.1	0.01	0.034
N6-Methyl-L-lysine	4.6	0.038	0.047
omega-Cyclohexylundecanoic acid	6.1	0.018	0.042
Phenylacetic acid	5.2	0.027	0.045
Propanoyl phosphate	4.2	0.044	0.047
Quinalphos	8	0.006	0.027
Retronecine	5.6	0.024	0.043
S-Acetyldihydrolipoamide	10.7	0.002	0.022
Stachydrine	10.2	0.003	0.026
Sulfite	5.7	0.02	0.042
Tetradecanoylcarnitine	5.1	0.029	0.046
Thr-Asp-Pro	4.3	0.043	0.047

117

118